

1 **Title:** Acid exposure disrupts mucus secretion and impairs mucociliary transport in neonatal
2 piglet airways

3
4 **One sentence summary:** Early life airway acidification produces mucus defects

5
6
7 **Authors:** Yan Shin J. Liao^{1#}, Shin Ping Kuan^{1#}, Maria V. Guevara^{1#}, Emily N. Collins^{1%}, Kalina
8 R. Atanasova^{1%}, Joshua S. Dadural¹, Kevin Vogt¹, Veronica Schurmann¹, Laura Bravo¹, Eda
9 Eken¹, Mariana Sponchiado¹, Leah R. Reznikov^{1*}

10
11 **Affiliations:**

12 ¹ Department of Physiological Sciences
13 University of Florida
14 Gainesville, FL 32610

15
16
17 *Contact Information: Leah Reznikov PhD
18 University of Florida
19 Department of Physiological Sciences
20 1333 Center Drive, PO Box 100144
21 Gainesville FL 32610
22 352 294 4059
23 Fax: 352 392 5145
24 Email: leahreznikov@ufl.edu
25

26
27
28
29
30 **# equal contribution**

31 **% equal contribution**

36 **ABSTRACT**

37 Tenacious mucus produced by tracheal and bronchial submucosal glands is a defining feature of
38 several airway diseases, including cystic fibrosis (CF). Airway acidification as a driving force of
39 CF airway pathology has been controversial. Here we tested the hypothesis that transient airway
40 acidification produces pathologic mucus and impairs mucociliary transport. We studied pigs
41 challenged with intra-airway acid. Acid had a minimal effect on mucus properties under basal
42 conditions. However, cholinergic stimulation in acid-challenged pigs revealed retention of
43 mucin 5B (MUC5B) in the submucosal glands, decreased concentrations of MUC5B in the lung
44 lavage fluid, and airway obstruction. To more closely mimic a CF-like environment, we also
45 examined mucus secretion and transport following cholinergic stimulation under diminished
46 bicarbonate and chloride transport conditions *ex vivo*. Under these conditions, airways from acid-
47 challenged pigs displayed extensive mucus films and decreased mucociliary transport. Pre-
48 treatment with diminazene aceturate, a small molecule with ability to inhibit acid detection
49 through blockade of the acid-sensing ion channel (ASIC) at the doses provided, did not
50 prevent acid-induced pathologic mucus or transport defects but did mitigate airway
51 obstruction. These findings suggest that transient airway acidification early in life has significant
52 impacts on mucus secretion and transport properties. Further, they highlight diminazene
53 acetate as an agent that might be beneficial in alleviating airway obstruction.

54

55

56

57

58

59 INTRODUCTION

60 Cystic Fibrosis (CF) is a life-shortening autosomal recessive disorder caused by mutations in the
61 gene encoding the *cystic fibrosis transmembrane conductance regulator (CFTR)*. CF airways are
62 distinguished by frequent infection, inflammation and adherent mucus. Over time, these factors
63 lead to progressive airway destruction and respiratory demise (6, 16, 41, 51). Several lines of
64 evidence suggest that airway mucus is abnormal in early CF disease (22, 61). For example,
65 pathologic findings in neonates with CF described bronchiole obstruction due to “thick” mucus
66 produced by the tracheal and bronchial submucosal glands (61). Hyperconcentration of mucins
67 due to excessive secretion of mucin5B (MUC5B) and mucin5AC (MUC5AC) cells has also been
68 reported (2). In porcine models of CF, a failure of mucus detachment from airway submucosal
69 glands was observed (22). Likewise, rats with CF display submucosal gland duct plugging prior
70 to onset of airway infection (5), whereas ferrets with CF show excessive mucus accumulation
71 even in a sterile airway environment (50).

72 The cause of abnormal mucus in CF has received significant attention (43). Numerous
73 mechanisms have been proposed, including dehydration of the airway (7, 19, 21, 32) and an
74 acidification of the airway caused by lack of CFTR-mediated bicarbonate transport (38, 40, 58).
75 Recently, Boucher and colleagues demonstrated that the proinflammatory cytokine IL-1 β
76 predominated the CF airway and correlated with increased expression of MUC5B (15). We
77 recently reported that acute airway acidification in neonatal piglets increased lung lavage
78 concentrations of IL-1 β and caused airway obstruction (45), however we did not examine mucus
79 transport or mucus secretion properties. Thus, here we tested the hypothesis that transient airway
80 acidification produces mucus with pathologic features and mucociliary transport defects.

81 Secondarily, we tested the hypothesis that pharmacological inhibition of acid detection would
82 mitigate acid-induced mucus deficits.

83 **MATERIALS AND METHODS.**

84

85 **Animals**

86 A total of 130 piglets (Yorkshire-Landrace, 2-3 days of age) were obtained from a commercial
87 vendor and fed commercial milk replacer (Liqui-Lean) and allowed a 24-hour acclimation period
88 prior to interventions. Data were collected from 17 separate cohorts of piglets across
89 approximately 1.5 - 2 years. At the conclusion of the experiments, animals were sedated with
90 ketamine (20 mg/kg), and xylazine (2.0 mg/kg), and intravenous propofol (2 mg/kg) (Henry
91 Schein Animal Health), followed by euthanasia with intravenous Euthasol (90mg/kg) (Henry
92 Schein Animal Health). The University of Florida Animal Care and Use Committee approved all
93 procedures. Care was in accordance with federal policies and guidelines.

94

95 **Airway Instillation**

96 After acclimation, piglets were anesthetized with 8% sevoflurane (Henry Schein). The piglets'
97 airways were accessed with a laryngoscope; a laryngotracheal atomizer (MADgic) was passed
98 directly beyond the vocal folds as previously described (45, 48) to aerosolize either a 500 µl
99 0.9% saline control or 1% acetic acid in 0.9% saline solution to the airway. This procedure
100 results in widespread distribution of aerosolized solutions throughout the piglet airway, including
101 the lung (11, 12).

102

103 **Chemicals and Drugs**

104 USP grade acetic acid (Fisher Scientific) was dissolved 0.9% saline to final concentration of 1%
105 and sterilized with a 0.22 μm filter (Millex GP). The pH of the 1% acetic acid solution measured
106 2.6 using an Accumet AE150 pH probe (Fisher Scientific). The estimated pH once applied to the
107 airway surface is \sim 6.6 to 6.8 (45). Acetyl-beta-methacholine-chloride (Sigma) was dissolved in
108 0.9% saline for intravenous delivery and *ex vivo* application; details about concentrations are
109 provided in respective experimental sections below. Diminazene aceturate (Selleckchem) was
110 dissolved in 0.9% saline containing 5% DMSO (Fisher Scientific).

111

112 **Diminazene aceturate delivery**

113 Approximately 30 minutes prior to airway instillations, piglets received an intramuscular
114 injection of either vehicle (5% DMSO + 95% 0.9% saline) or vehicle containing 17.5 mg/ml
115 (\sim 33.7 millimolar) diminazene aceturate. Diminazene aceturate was dosed at 3.5 mg/kg. This
116 dose was chosen based upon previous studies showing efficacy in trypanosome infections in
117 dogs (35) and is below the reported dose required to affect angiotensin converting enzyme 2
118 (ACE2) (8, 42). Using a conversion chart for dogs (1), we estimated the body surface area of a 2-
119 3 kg piglet to be 0.16-0.21 m^2 . Based upon this conversion, the estimated final drug molarity in
120 the pig body was \sim 9 μM , which should provide near 100% block of ASIC1a, as it is 3 fold
121 greater than the IC₅₀ of 3 μM (10, 29). The time point of 30 minutes prior to instillation was
122 selected based upon previous studies showing peak serum concentrations at 15 minutes and peak
123 interstitial fluid concentrations at 3 hours in adult rabbits (17).

124

125 **Bronchoalveolar lavage and ELISA**

126 Following euthanasia, the caudal left lung of each piglet was excised and the main bronchus
127 cannulated; three sequential 5 ml lavages of 0.9% sterile saline were administered as previously
128 described (45, 48). The recovered material was pooled, spun at 500 X g, and supernatant stored
129 at -80°C. A porcine MUC5AC (LSBio, LS-F45847-1) and porcine MUC5B (LSBio, LS-F45852-
130 1) ELISA was performed according to the manufacturer's instructions in duplicate. The ELISA
131 was read using a filter-based accuSkan FC micro photometer (Fisher Scientific). The limits of
132 sensitivity were <0.188 ng/ml and < 0.375 ng/ml for MUC5AC and MUC5B, respectively. The
133 intra-assay and inter-assay coefficient of variability were respectively <6.1% and <5.2% for
134 MUC5AC and <6.5% and <5.9% for MUC5B.

135

136 **Histology**

137 Lung tissues were fixed in 10% neutral buffered formalin (~7-10 days), processed, paraffin-
138 embedded, sectioned (~4 µm) and stained with Periodic-acid-Schiff stain (PAS) to detect
139 glycoproteins as previously described (45, 48). Digital images were collected with a Zeiss Axio
140 Zoom V16 microscope. Indices of obstruction were assigned as previously described (45, 48).

141

142 **Immunofluorescence in tracheal cross sections**

143 1-2 tracheal rings were removed post-mortem and embedded in Peel-A-Way embedding molds
144 containing Tissue-Tek OCT (Electron Microscopy Sciences). Molds were placed in a container
145 filled with dry ice until frozen and stored at -80 °C long-term. Tissues were sectioned at a
146 thickness of 10 µm and mounted onto SuperFrost Plus microscope slides (ThermoFisher
147 Scientific). Storage until immunofluorescence also occurred at -80 °C. We used
148 immunofluorescence procedures similar to those previously described (45, 47). Briefly,

149 representative cross-sections from a single cohort of pigs were selected and fixed in 2%
150 paraformaldehyde for 15 minutes. Tissues were then permeabilized in 0.15% Triton X-100,
151 followed by blocking in PBS Superblock (ThermoFisher Scientific) containing 2-4% normal
152 goat serum (Jackson Laboratories). Tissues were incubated with primary antibodies for 2 hours
153 at 37 °C. Tissues were washed thoroughly in PBS and incubated in secondary antibodies for 1
154 hour at room temperature. Tissues were washed and a Hoechst stain performed as previously
155 described (45). A 1:10 glycerol/PBS solution was used to cover the sections and cover glass
156 added. Sections were imaged on a Zeiss Axio Zoom V16 microscope. Identical microscope
157 settings within a single cohort of piglet tracheas were used and applied. Three to five images
158 encompassing the posterior, anterior, and lateral surfaces of the trachea were taken. Images were
159 exported and analyzed using ImageJ. The trachea surface epithelia and entire submucosal gland
160 regions were traced and the mean signal intensity MUC5B and MUC5AC recorded. Background
161 signal intensity was measured and subtracted manually. The final signal intensities were
162 averaged to identify a mean signal intensity for MUC5B and MUC5AC per sub-compartment for
163 each piglet. To analyze the amount of the trachea lumen that was ciliated, three images of the
164 trachea were assessed and the length of the epithelia that was ciliated was divided by the total
165 length of the epithelia and percent reported. The percent of each image was averaged and
166 reported per each piglet.

167

168 **Antibodies and lectins**

169 We used the following anti-mucin antibodies: rabbit anti-MUC5B (1:500; Santa Cruz, Cat.#
170 20119) and mouse anti-MUC5AC (clone 45M1) (1:1,000, ThermoFisher Scientific, Cat #
171 MA512178), mouse anti-acetyl alpha tubulin, clone 6-11B-1, 1:500 (EMD Millipore,

172 MABT868) (28), followed by goat anti-rabbit and goat anti-mouse secondary antibodies
173 conjugated to Alexa-Fluor 488 or 568 (ThermoFisher Scientific, 1:1,000 dilution). We used
174 WGA-rhodamine (Vector Laboratories) and Jacalin-FITC (Vector Laboratories) at 1:1,000
175 dilution. Tracheas were submerged in PBS and visualized using a Zeiss Axio Zoom V16
176 microscope.

177

178 ***In vivo* methacholine and ventilation**

179 We have previously described the ventilation and *in vivo* methacholine procedures in piglets (45,
180 48). Briefly, 48 h post instillation, animals were anesthetized with ketamine (20 mg/kg), and
181 xylazine (2.0 mg/kg), and intravenous propofol (2 mg/kg) (Henry Schein Animal Health). A
182 tracheostomy was performed, and a cuffless endotracheal tube (Covidien, 3.5–4.0 mm OD) was
183 placed. Piglets were connected to a flexiVent system (SCIREQ); paralytic (rocuronium bromide,
184 Novaplus) was administered. Piglets were ventilated at 60 breaths/min at a volume of 10 ml/kg
185 body mass. Methacholine was administered intravenously in approximately ~3 min intervals
186 with increasing concentrations (in mg/kg): 0.25, 0.5, 1.0, 1.5, 2.0. Piglets were ventilated to
187 ensure animal well-being and patency of airway tissues during cholinergic challenge.

188

189 **Mucus secretion assay *ex vivo***

190 We adopted methods described by Ostedgaard et al (36). Briefly, 3-4 rings of trachea were
191 removed post-mortem and the outside of the tracheas were wrapped in gauze soaked with 5 ml of
192 the following: 135 mM NaCl, 2.4 mM K₂HPO₄, 0.6 mM KH₂PO₄, 1.2 mM CaCl₂, 1.2 mM
193 MgCl₂, 10 mM dextrose, 5 mM HEPES, pH 7.4 (NaOH), 1.5 mg/ml of methacholine, and 100
194 μM bumetanide. We determined that the amount of methacholine the tissue was exposed to was
195 0.15 mgs total (e.g., external surface of the trachea is covered by approximately 100 μl). Thus,

196 the methacholine dose delivered to the trachea was 0.15 mg/4.71 cm² (tissue dimensions of
197 trachea: radius = 0.5 cm, height = 1.5 cm). Using a conversion chart for dogs (1), we estimated
198 the body surface area of a 2-3 kg piglet to be 0.16-0.21 m². Therefore, the estimated dose of
199 methacholine delivered to the tissue was ~6-7 fold higher than the cumulative *in vivo* dose of
200 methacholine to account for diffusion of methacholine across tissues layers and in the absence of
201 blood circulation. Tracheas were then placed in a temperature-controlled humidified incubator
202 for 3 hours. Following stimulation, tracheas were fixed overnight in 4% paraformaldehyde and
203 permeabilized for 30 minutes using a triton solution (0.15%), followed by blocking in
204 SuperBlock PBS. Jacalin-FITC and wheat-germ agglutinin-rhodamine were used to visual mucus
205 (3, 36) and incubated overnight with tracheas at concentration of 1:1,000. Tracheas were then
206 washed, cut upon the posterior surface, and pinned to wax covered petri-dishes followed by
207 submersion in PBS. Tracheas were imaged with Zeiss Axio Zoom V16 posterior to anterior
208 using identical microscope settings. Images were assigned scoring indices for sheet formation
209 and strand formation by two observers blinded to conditions. The number of dilated submucosal
210 gland ducts was also measured by two observers blinded to conditions. Scoring for sheet
211 formation follows: 1 = no sheet formation; 2 = 1-25% of image field shows sheet formation; 3 =
212 26-50% of image field shows sheet formation; 4 = 51-75% of image field shows sheet formation;
213 5 = 76-100% of image field shows sheet formation. Sheet formation was defined as the loss of
214 discrete cellular packets of mucus. Secondary analysis and validation of scoring was performed
215 with IMARIS software (detailed below). Scoring for strand formation was similar to sheet
216 formation. Scoring for strand formation follows: 1 = no strand formation; 2 = 1-25% of image
217 field shows 3 = 26-50% of image field shows a strand; 4 = 51-75% of image field shows a
218 strand; 5 = 76-100% of image field shows a strand. Secondary analysis consisting of tracing the

219 strand area and expressing it a percentage of the total image field of view was also performed on
220 a subset of images in ImageJ.

221

222 ***Ex vivo* mucus transport assays**

223

224 Mucociliary transport was measured using methods similar to those described by Hoegger et al
225 (22). Briefly, 3 rings of tracheas were submerged in 5 ml of prewarmed solution containing the
226 following: 138 mM NaCl, 1.5 mM KH₂PO₄, 0.9 mM CaCl₂, 0.5 mM MgCl₂, 2.67 mM KCl, 8.06
227 mM Na₂HPO₄·7H₂O, 10 mM HEPES, pH 7.4 (NaOH), and 100 μM bumetanide. Tracheas were
228 placed onto a heated stage and kept at 37 °C. Images were acquired every 1 minute for 35
229 minutes. After 5 minutes of baseline measurements, methacholine was administered directly into
230 the solution covering the basolateral and apical sides of tracheas at a dose of 0.004 mg/ml. This
231 dose matched the estimated accumulative dose of methacholine administered to piglets *in vivo*
232 (*e.g.*, 3.75 mg/kg = 3.75 mg/L = 0.00375 mg/ml). Mucus transport was assessed for an additional
233 30 minutes, with the exception of one set of tracheas, in which only an additional 25 minutes was
234 measured. In one additional sample, the microscope malfunctioned after 5 minutes of recording
235 post methacholine stimulation. IMARIS software was used to track mucus transport across time
236 measured. Details about IMARIS software and processing are highlighted below.

237

238 **IMARIS computer-assigned particles for measurement of mucus transport and mucus** 239 **sheet formation**

240 Computer particles based upon signal intensity above background were automatically generated
241 with IMARIS software (Bitplane). The particles were then tracked through time using a custom
242 IMARIS algorithm that utilized principles of the well-validated algorithms published by

243 Jaqaman and colleagues (24). For each trachea, the average mean speeds of the computer-
244 assigned particles were reported. The length of the particle track was also computed
245 automatically and the mean track length of all the particles per trachea were calculated and
246 reported. For determination of sheet formation, an image was chosen at random from a subset of
247 tracheas stained with lectins. Particles were assigned to the images automatically as described
248 above. The number of particles (representing the jacalin-labeled mucus with intensity above
249 background) were reported. In tracheas that exhibit robust mucus sheet formation, the number of
250 computer-assigned particles is decreased due to a loss of discreet cellular packets of jacalin-
251 labeled mucus.

252

253 **Statistical analysis**

254 Our previous work indicated that airway acidification elicited sex-independent airway
255 obstruction (45). Thus, in the current study, we hypothesized that airway acidification would
256 have sex-independent effects on airway mucus and mucociliary transport. To test this prediction,
257 we initially performed a two-way ANOVA (sex as one factor, treatment as the other factor), but
258 observed no significant interactions between sex and treatment, indicating that sex did not affect
259 the response to treatments. Thus, stratification based upon sex was not strongly justified (59),
260 and therefore we grouped the data to better represent the population. Two-way ANOVA analyses
261 stratified by sex are available in Table 1. For parametric data that compared four groups, we used
262 a two-way ANOVA test, with treatment as one factor and drug as the other factor, followed by a
263 Sidak multiple comparison test. Post-hoc multiple comparison tests were run in a classic 2x2
264 manner, comparing cell means for across rows and columns. Similar to our previous studies, for
265 non-parametric data that compared four groups, we used a one-way ANOVA (Kruskal-Wallis)
266 test followed by Dunn's multiple comparison test (45, 48). For all experiments, we reported the

267 following post-hoc comparisons, due to relevance of the questions being asked in our study: acid
268 vs saline; acid vs acid + diminazene aceturate, and saline vs saline + diminazene aceturate. For
269 analyses that compared two groups, we used a two-tailed unpaired Student's t-test. All tests were
270 carried out using GraphPad Prism 7.0a. Statistical significance was determined as $P < 0.05$.

271

272 **RESULTS**

273 **Airway mucin secretion in acid-challenged piglet is largely unaffected under basal** 274 **conditions**

275 We performed multi-level analyses of the major secretory gel-forming mucins, MUC5AC and
276 MUC5B (20, 27). We examined basal secretion by measuring the amount of MUC5AC and
277 MUC5B in the bronchoalveolar lavage fluid. Detectable levels of proteins were found in all
278 treatment groups. No statistically significant differences were noted in MUC5AC concentrations
279 (treatment, $F_{1,27} = 2.63$, $p = 0.12$; drug, $F_{1,27} = 1.86$, $p = 0.18$; interaction, $F_{1,27} = 1.12$, $p = 0.29$,
280 Figure 1A). Post hoc comparisons indicated a trend for decreased concentrations of MUC5B in
281 acid-challenged piglets ($p = 0.068$) compared to saline-treated controls, whereas decreased
282 concentrations of MUC5B were observed in saline-treated animals that received diminazene
283 aceturate compared to saline-treated animals that did not receive diminazene aceturate
284 (treatment, $F_{1,27} = 21.66$, $p < 0.0001$; drug, $F_{1,27} = 37.9$, $p < 0.0001$; interaction, $F_{1,27} = 67.11$, p
285 < 0.0001 , Figure 1B).

286

287 Bronchoalveolar lavage fluid is limited in that it primarily captures non-adherent proteins and is
288 a mixed fluid retrieved from alveolar and bronchial spaces. Therefore, we measured MUC5AC
289 and MUC5B protein expression in tracheal cross sections using antibody-specific labeling and

290 signal intensity analyses (15). We observed no significant differences in MUC5AC signal
291 intensity within and on the tracheal surface across treatment groups (treatment, $F_{1,54} = 1.98$, $p =$
292 0.17 ; drug, $F_{1,54} = 0.84$, $p = 0.36$; interaction, $F_{1,54} = 3.64$, $p = 0.06$, Figure 1C). Main effects of
293 treatment ($F_{1,54} = 15.00$, $p = 0.0003$) and drug ($F_{1,54} = 12.11$, $p = 0.001$) were observed for
294 MUC5B signal intensity on the tracheal surface, but no interactions were noted ($F_{1,54} = 0.99$, $p =$
295 0.32 , Figure 1D). Analysis of MUC5AC expression in the submucosal glands revealed a
296 significant main effect of treatment ($F_{1,54} = 8.69$, $p = 0.0047$), but no effect of drug ($F_{1,54} = 0.29$,
297 $p = 0.59$) or interaction ($F_{1,54} = 1.23$, $p = 0.27$) were noted (Figure 1E). Similarly, analysis of
298 MUC5B expression in the submucosal glands revealed a significant main effect of treatment ($F_{1,$
299 $54 = 5.84$; $p = 0.019$), but no effect of drug ($F_{1,54} = 0.22$, $p = 0.64$) or interaction ($F_{1,54} = 1.66$, $p =$
300 0.20) was observed (Figure 1F). These data suggested that acid challenge minimally affected
301 basal mucin production and secretion in the airway.

302

303 **MUC5B secretion in response to cholinergic stimulation is modified in acid-challenged** 304 **piglet airways**

305 Previous studies suggested that CF airways are characterized by abnormal submucosal gland
306 secretion and ductal plugging. Thus, we stimulated submucosal gland secretion by administering
307 the cholinergic agonist methacholine and assessed mucin secretion. No significant differences in
308 MUC5AC concentrations in the bronchoalveolar lavage fluid from methacholine-stimulated
309 piglets were found (treatment, $F_{1,23} = 0.68$, $p = 0.42$; drug, $F_{1,23} = 2.05$, $p = 0.17$; interaction, $F_{1,$
310 $23 = 1.68$, $p = 0.21$, Figure 2A). In contrast, MUC5B concentrations were significantly decreased
311 in acid-challenged piglets compared to saline-treated controls (treatment, $F_{1,23} = 11.13$, $p =$
312 0.0029 ; drug, $F_{1,23} = 50.97$, $p < 0.0001$; interaction, $F_{1,23} = 59.55$, $p < 0.0001$, Figure 2B).

313 Treatment with diminazene aceturate did not prevent acid-induced defects (Figure 2B) but did
314 decrease MUC5B concentrations in saline-treated pigs compared to saline-treated pigs without
315 diminazene aceturate (Figure 2B).

316

317 Assessment of MUC5B and MUC5AC expression in tracheal cross sections revealed no
318 statistically significant effect of acid on surface MUC5AC (treatment, $F_{1,31} = 1.083$, $p = 0.31$;
319 drug, $F_{1,31} = 3.48$, $p = 0.072$; interaction, $F_{1,31} = 0.71$, $p = 0.41$, Figure 2C). Main effects of
320 treatment ($F_{1,31} = 12.55$, $p = 0.013$) and drug ($F_{1,31} = 11.04$, $p = 0.0023$), as well as an
321 interaction ($F_{1,31} = 15.46$, $p = 0.0004$) were noted for MUC5B surface expression (Figure 2D).
322 However, post hoc comparisons revealed no statistically significant differences between acid-
323 challenged pigs and saline-challenged pigs (Figure 2D). In contrast, saline-challenged piglets
324 treated with diminazene aceturate showed a significant elevation in surface MUC5B compared to
325 saline-challenged pigs without diminazene aceturate treatment (Figure 2D). No differences were
326 observed in MUC5AC labeling in the submucosal gland (treatment, $F_{1,31} = 3.99$, $p = 0.055$; drug,
327 $F_{1,31} = 0.002$, $p = 0.961$; interaction, $F_{1,31} = 0.342$, $p = 0.563$, Figure 2E). In contrast, MUC5B
328 labeling tended to be greater in the submucosal gland of acid-challenged piglets and was
329 significantly elevated in the submucosal glands of saline-treated piglets provided diminazene
330 aceturate (treatment, $F_{1,31} = 1.46$, $p = 0.236$; drug, $F_{1,31} = 5.69$, $p = 0.0234$; interaction, $F_{1,31} =$
331 21.25 , $p < 0.0001$, Figure 2F). Combined, these data suggested three key findings: 1) acid
332 challenge impacted stimulated submucosal gland secretion; 2) diminazene aceturate did not
333 prevent the effects of acid; and 3) in the absence of acid challenge, diminazene aceturate
334 modified mucus secretion properties.

335

336 **Diminazene aceturate mitigates acid-induced mucus obstruction**

337 Obstruction of the small airways is common in CF, and alterations in mucus biophysical
338 properties and composition can lead to airway obstruction. Thus, we examined the small airways
339 for evidence of obstruction using standard histological techniques (45). Similar to our previous
340 studies (45), we found that acid challenge induced airway obstruction under both basal ($F_{3,60} =$
341 13.81 ; $p = 0.0032$, Figure 3A-3E) and methacholine-stimulated conditions ($F_{3,31} = 10.21$; $p =$
342 0.0169 , Figure 4A-4E). Diminazene aceturate significantly attenuated airway obstruction in both
343 conditions (Figure 3, Figure 4).

344

345 **Intra-airway acid induces formation of mucus sheets and mucus strands**

346 All of our *in vivo* studies were performed under normal physiologic conditions. However, in CF,
347 there is a diminished bicarbonate and chloride transport. Thus, to more closely mimic a CF
348 environment, we investigated mucus morphology and secretion properties *ex vivo* in tracheal
349 segments stimulated with methacholine under diminished bicarbonate and chloride transport
350 conditions. As a surrogate marker for MUC5AC and MUC5B, we stained mucus with jacalin
351 (36) and wheat germ agglutinin (WGA)(36), respectively.

352

353 In saline-treated piglet airways, mucus was found in discreet packets that decorated the surface
354 like ornaments (Figure 5A). In contrast, mucus in acid-challenged piglets formed film-like sheets
355 (Figure 5B). Acid-challenged pigs showed greater mucus sheet formation for jacalin-labeled
356 mucus ($F_{3,53} = 34.69$; $p < 0.0001$, Figure 5E). A main treatment effect was observed for WGA-
357 labeled mucus ($F_{3,53} = 53.31$; $p = 0.0011$, Figure 5F) but post-hoc comparisons revealed no
358 significant differences between acid-challenged and saline-challenged pigs. In a smaller cohort

359 of samples, we also assessed mucus sheet formation using IMARIS software and found a
360 decrease in the number of discrete mucus particles in acid-challenged pigs compared to saline-
361 treated controls ($t_{16} = 4.416$, $p = 0.0004$, Figure 5G). Diminazene aceturate did not significantly
362 alter or prevent the formation of sheet-like structures (Figure 5C-E).

363
364 Mucus strands emanating from submucosal glands are characteristic of CF airways (14, 36).
365 Thus, we examined tracheal segments stimulated *ex vivo* with methacholine for strand formation
366 (Figure 6). A significant main effect of treatment was observed for the abundance of strands
367 formed by mucus labeled with jacalin ($F_{3, 53} = 13.42$; $p = 0.0038$, Figure 6E), but post-hoc
368 comparisons revealed no significant differences between acid-challenged and saline-challenged
369 pigs. However, a significant increase in strand formation for WGA-labeled mucus was observed
370 in acid-challenged piglets compared to saline-treated controls ($F_{3, 53} = 18.62$; $p = 0.0003$, Figure
371 6F). In a smaller cohort of samples, we performed a secondary analysis that consisted of tracing
372 the strand area manually in image J and expressing it as a percentage of the total image field of
373 view. Consistent with our scoring method, manual tracing also indicated significantly more
374 strands in acid-challenged piglets compared to saline-treated controls ($t_{16} = 2.22$, $p = 0.0412$,
375 Figure 6G). Diminazene aceturate did not significantly alter mucus strand formation (Figure 6C-
376 F).

377
378 Dilated submucosal gland ducts, due to plugging and obstruction of the submucosal gland, are
379 commonly observed in CF airways (61). Thus, we also examined the tracheal surfaces for the
380 presence of dilated submucosal gland duct openings. Submucosal gland duct openings were only
381 marginally visible in saline-treated piglets (Figure 7A). In stark contrast, acid-challenged piglets

382 displayed a significant elevation in dilated submucosal gland duct openings (Figure 7B).

383 Statistical analysis revealed a main effect of treatment ($F_{1,53} = 36.45$; $p < 0.0001$), but no effect
384 of drug ($F_{1,53} = 2.72$; $p = 0.11$) or interaction ($F_{1,53} = 2.72$; $p = 0.11$). The lack of interaction
385 precluded any post hoc testing between groups.

386

387 **Mucociliary transport is impaired in acid-challenged airways**

388 CF airways are distinguished by impaired mucociliary transport (5, 22, 25, 34). Thus, we studied
389 freshly excised tracheal segments stimulated with methacholine under diminished bicarbonate
390 and chloride transport conditions. We assessed mucociliary transport using methods developed
391 by Hoegger and colleagues (22), in which tracheas are submerged in a physiologic solution
392 containing fluorescent nanospheres that bind and attach to mucus, allowing for real-time
393 visualization of mucus production and movement. To measure the movement of fluorescently-
394 labeled mucus, we utilized IMARIS computer assigned particle-tracking that uses validated
395 algorithms (24) (Figure 8A-E). We found that the average speed of mucus was decreased in acid-
396 challenged pig airways (treatment, $F_{1,60} = 3.69$, $p = 0.059$; drug, $F_{1,60} = 3.03$, $p = 0.087$;
397 interaction, $F_{1,60} = 4.002$, $p = 0.05$, Figure 8F). Because speed is equal to distance over time, we
398 also examined computer assigned particle track length and found it was decreased in acid-
399 challenged airways (treatment, $F_{1,60} = 2.68$, $p = 0.107$; drug, $F_{1,60} = 0.802$, $p = 0.3740$;
400 interaction, $F_{1,60} = 6.198$, $p = 0.0156$, Figure 8G). Finally, we noted that under submerged
401 conditions, there was very little mucus that accumulated on the airway surface in acid-challenged
402 pigs. Therefore, at the conclusion of the experiment, we measured the signal intensity of
403 fluorescently labeled mucus on the airway surface (Figure 8H). We found a main effect of

404 treatment ($F_{1,60} = 18.4$, $p < 0.0001$), but no effect of drug ($F_{1,60} = 0.4256$, $p = 0.5166$) or an
405 interaction ($F_{1,60} = 0.9036$, $p = 0.3459$), thus precluding any post hoc comparisons.

406

407 Because mucociliary transport can also be decreased due to defects in cilia number and/or
408 function, we also measured the percent of the trachea lumen that was ciliated using antibody
409 labeling (Figure 9A-D). We found a main effect of treatment ($F_{1,52} = 12.92$, $p = 0.0007$), but no
410 effect of drug ($F_{1,52} = 0.0499$, $p = 0.824$), or an interaction ($F_{1,52} = 0.0625$, $p = 0.8036$), were
411 observed (Figure 9E).

412

413 **DISCUSSION**

414 Early in CF pathogenesis, the airway is acidic (4, 5, 38). Although mucus abnormalities precede
415 airway infection and inflammation (5, 15, 22), whether transient airway acidification is sufficient
416 to produce pathologic mucus and decrements in mucociliary transport is controversial. Thus, we
417 interrogated the effect of early life airway acidification on mucus properties by studying neonatal
418 piglets challenged with intra-airway acid or saline control. Secondly, to investigate potential
419 mechanisms, we blocked detection of acid with diminazene aceturate (53).

420

421 Our data showed a marginal effect of transient acidification on basal mucin expression and
422 secretion under physiologic conditions. Upon *in vivo* methacholine stimulation, acid-challenged
423 pigs had less MUC5B in the bronchoalveolar lavage fluid and tended to have more MUC5B
424 retained in the submucosal gland compared to saline-treated controls, suggesting a defect at the
425 level of the submucosal gland. To more closely mimic a CF-like environment, we investigated
426 mucus secretion properties under diminished bicarbonate and chloride transport conditions.

427 Under these conditions, we observed abnormal mucus secretion in acid-challenged pig airways,
428 characterized by extensive mucus sheets and mucus strands. These features are similar to those
429 described in newborn CF pig airways (36, 58). Acid-challenged pigs also displayed decreased
430 mucociliary transport under diminished bicarbonate and chloride transport conditions. Thus,
431 combined, these data suggest that transient airway acidification produces abnormal mucus
432 secretion and transport, mimicking several features of CF.

433

434 Direct measurements of airway pH in children with CF have suggested that pH is not different
435 compared to children that do not have CF (33, 54), yet other studies suggest that the airways are
436 acidified in human neonates with CF (4). These findings have raised controversy whether
437 acidification is an initiating factor in CF pathogenesis. In our model, the acidification procedure
438 we utilize leads to a mild decrement in airway pH (45), resulting in airway pH values similar to
439 what has been reported in animal models of CF (58). While we did not observe a significant
440 increase in mucin production that others have reported in CF (15), we did find other similarities,
441 including evidence for defective submucosal gland secretion, airway obstruction and impaired
442 mucociliary transport (5, 22, 52, 61). It is likely that the cause of decreased mucociliary transport
443 was multifactorial, with both a loss of cilia and change in mucus secretion contributing. It is also
444 possible that acidic pH caused a sustained change in mucus viscosity (58), which could also
445 decrease mucociliary transport.

446

447 To interrogate potential mechanisms, we studied diminazene aceturate. Diminazene aceturate is a
448 widely used drug for the treatment of protozoan diseases with reportedly minimal adverse side
449 effects (13). Its low cost and availability in numerous regions of the world make it an attractive

450 drug. Diminazene aceturate blocks the acid-sensing ion channel 1a (ASIC1a) (53), which is
451 present in nerves innervating the airway (18, 30), and throughout the central nervous system
452 (39). Since airway nerves are critical in detecting noxious stimuli and regulating mucus
453 secretion, we hypothesized that detection of acid through ASIC1a might be critical in our model.

454

455 We found that diminazene aceturate had a negligible effect in preventing acid-induced mucus
456 defects, despite being used at doses known to inhibit ASIC1a (10, 29). In contrast, diminazene
457 aceturate treatment in saline-challenged controls lead to a significant increase in MUC5B on the
458 airway surface, but less MUC5B in the bronchoalveolar lavage fluid. Although unbuffered saline
459 is acidic (44, 46), our previous studies showed that application of unbuffered saline to the apical
460 surface of porcine airway epithelial cells *in vitro* had a negligible effect on airway surface liquid
461 pH (45). However, we cannot exclude the possibility that unbuffered saline induces a transient
462 activation of ASIC1a in the airway, as current techniques may underestimate the change in pH. If
463 true, then the effect of diminazene aceturate on MUC5B in saline controls is potentially via
464 inhibition of ASICs, although other mechanisms could also be involved (8, 42).

465

466 The lack of effect in acid-challenge conditions suggests that either the dosing or delivery of
467 diminazene aceturate was suboptimal. For example, our previous studies demonstrated that acid
468 application to porcine airway epithelial cells *in vitro* produced a transient acidification of the
469 airway surface liquid from 7.5 to ~6.6 (45). Previous studies showed that the ASIC1a decay in
470 response, or desensitization, is pH-dependent, with slower desensitization correlating with proton
471 concentration (31). Specifically, when ASIC1a was subjected to a drop in pH from 7.4 to 6.6,
472 subsequent application of solutions of pH 7.2 and 7.4 prolonged the desensitization period

473 compared to solutions of pH 7.6 and 8.0. This property translates into prolonged channel
474 activation at low proton concentrations (31). This might be particularly important in our
475 paradigm, in which pH likely returns to baseline over the course of 10 minutes (45). Therefore, it
476 is possible that we underestimated the dose required to cause effective and sustained blockade of
477 ASIC1a in the trachea, which is expected to receive a greater and more homogeneous exposure
478 to acid (45). Alternatively, this finding might suggest that ASIC1a is not involved in acid-
479 mediated mucus defects at the trachea level.

480

481 We observed a strong protective effect of diminazene aceturate in the intrapulmonary airways. It
482 is possible that ASIC1a is more concentrated in the small airways compared to the large airways.
483 The lack of commercially available antibodies that detect ASIC1a in the pig preclude
484 investigations focused on addressing this question. Although we are not certain of the
485 mechanisms by which potential activation of ASICs in the intrapulmonary airways could lead to
486 airway obstruction, our previous work illustrated that this acid-challenge model induces neural
487 remodeling at the level of nodose ganglia and in the brainstem. These changes were associated
488 with airway obstruction and predicted to involve A δ and c-fibers (26, 45, 60). Consistent with
489 that, we previously found that elimination of ASIC1a in mice disrupted sensory nerve function,
490 leading to a decreased amount of the neuropeptide substance P in the lung lavage fluid of
491 ovalbumin-sensitized mice compared to wild-type controls (47). Recent work demonstrates that
492 substance P in vagal sensory neurons drives mucus cell metaplasia (57). Therefore, if ASICs
493 were indeed involved in the acid-mediated airway obstruction, then it is conceivable that
494 substance P in c-fibers innervating the intrapulmonary airways played a role. Additionally,
495 although our previous work suggests negligible expression of ASIC1a in murine airway cells

496 (45), it is possible that ASIC1a is expressed in non-neuronal cells in the small airways of the pig.
497 An additional consideration is that the effects of diminazene aceturate were not ASIC1a-related
498 at all and perhaps due to off-target effects, such as activity on the (ACE2) (8, 42). Although the
499 diminazene aceturate dose used in this study was below the reported dose required to cause
500 activity on ACE2, it is a possibility that we must consider.

501
502 We previously examined inflammation extensively in acid-challenged piglets using
503 inflammatory-directed gene arrays and ELISAs, and found evidence for transcriptional
504 inflammation, as well as an elevation in IL-1 β protein levels (45). Recently Boucher and
505 colleagues reported that IL-1 β predominates the CF airway and correlates with mucin production
506 (9). Thus, it is possible that IL-1 β contributes to some of the acid-mediated defects we report
507 here.

508
509 We found a main effect of acidification on cilia abundance in the trachea. Although we did not
510 investigate mechanisms responsible for this observation, deciliation in response to other airway
511 irritants, such as viral infection and smoke, have been reported (55). Similarly, epithelial damage
512 following severe bronchospasm has also been reported (37). Thus, it is possible that both
513 chemical (pH) and mechanical (bronchoconstriction) forces contributed to the observed effect of
514 acidification on airway ciliation.

515
516 Our studies demonstrated that acidification impaired mucus secretion and decreased mucociliary
517 transport. While we do not know whether a change in the biophysical properties of
518 mucins/mucus contributed, strong evidence suggests that mucin folding, secretion, and viscosity

519 are pH-dependent (49, 58) . For example, recently Hughes and colleagues reported that when
520 MUC5B is subjected to an acidic pH and high calcium environment, it forms dense structures
521 (23). Such structures are likely to impact the mucus barrier and modify the transition from a
522 condensed form of mucin to a more expanded form of mucin. However, biophysical changes are
523 typically reversible and flexible (23, 49, 58). Thus, in our experimental model, it is anticipated
524 that an effect of acidification on mucin/mucus biophysical properties would have occurred
525 acutely during the initial exposure to acid and likely reversed by the time the studies were
526 conducted (48 hours later). This suggests that perhaps the effect of acidification on mucus
527 secretion and mucus transport in our studies was not due to an acute change in biophysical
528 properties. Alternatively, if biophysical properties were altered in our model, then they might
529 have been more long-term or sustained.

530

531 Our study has limitations. We did not assess mucus secretion under basal and stimulated
532 conditions within the same subject. This was largely due to the inability to take airway samples
533 from a subject before and after methacholine stimulation. Further, our study was transient and
534 therefore lacked information regarding long-term consequences of airway acidification.
535 However, the transient nature of our study might also be an advantage, because it allowed for the
536 effects of acidification to be isolated from potential secondary complications, such as infection
537 and/or prolonged inflammation. We also did not identify a mechanism responsible for acid-
538 mediated defects in mucus secretion and mucus transport, but our studies highlight the
539 submucosal gland as a target of airway acidification. Although not measured here, it is possible
540 that a reduction in ciliary beat frequency, either due directly to acid (56), or secondarily due to
541 changes in mucus composition, contributes. We also did not study mucus transport under normal

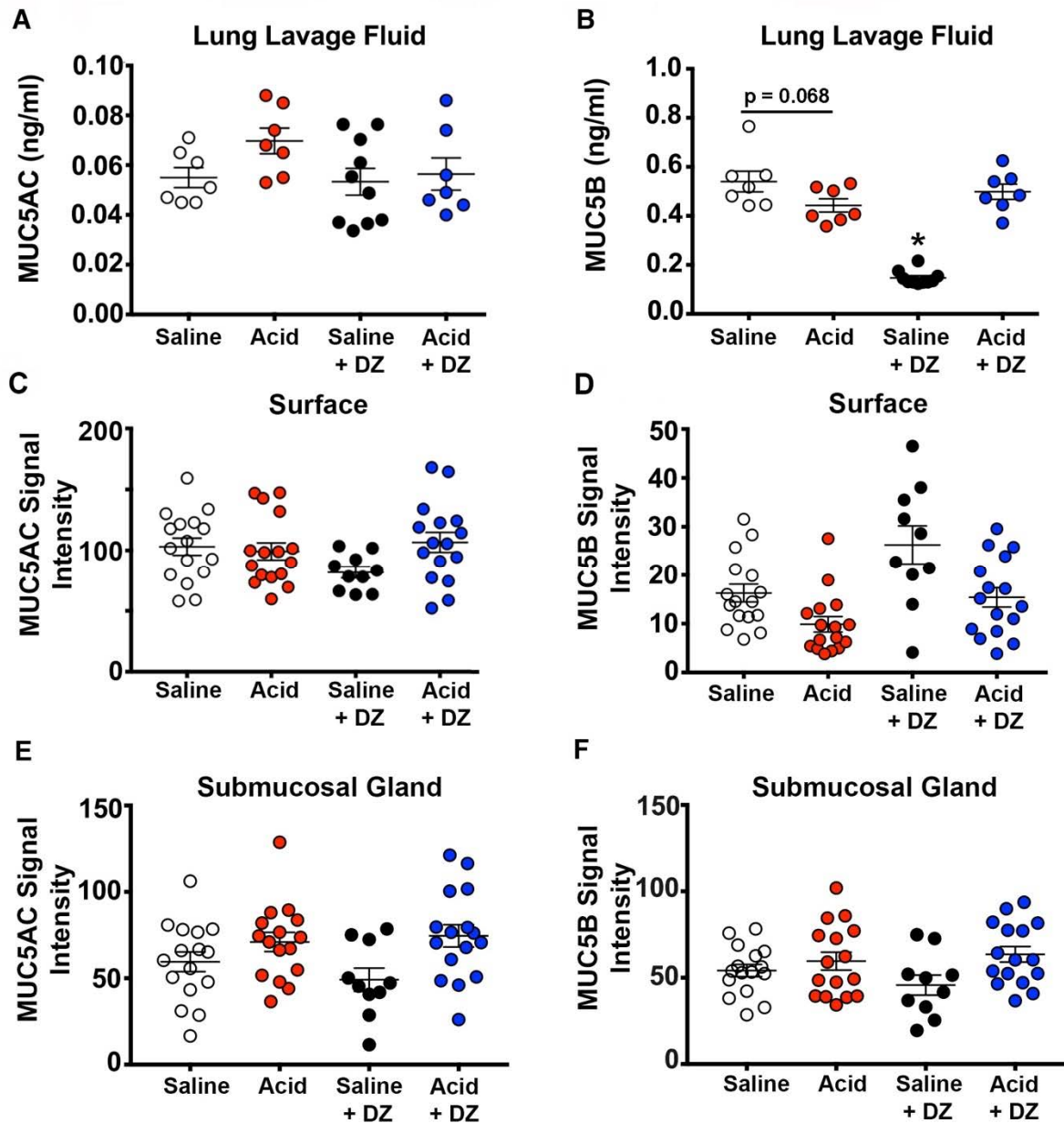
542 chloride and bicarbonate conditions; thus, we cannot make any conclusions regarding the
543 specificity of acidification in driving airway pathology in a CF-like environment. Finally, as
544 mentioned above, we did not study the biophysical or biochemical properties of mucus (e.g.,
545 glycosylation, viscosity); future studies focused on these qualities will be of value.

546

547 In summary, early life airway acidification produced mucus with pathologic features, airway
548 obstruction, and decreased mucociliary transport. Diminazene aceturate mitigated acid-induced
549 airway obstruction. Thus, these findings suggest that even transient airway acidification early in
550 life might have profound impacts on mucus secretion and transport properties. Further, they
551 highlight diminazene aceturate as a potential agent beneficial for alleviating some features of CF
552 airway disease.

553

554 **Figures and Figure Legends**



555
 556 **Fig. 1. Mucin in piglet airways under basal conditions.** Bronchoalveolar lavage fluid
 557 concentrations of MUC5AC (A) and MUC5B (B). MUC5AC and MUC5B staining signal
 558 intensity of the surface epithelia (C, D) and submucosal gland (E, F). For panels A and B, n = 7
 559 saline-challenged piglets (4 females, 3 males), n = 7 acid-challenged pigs (4 females, 3 males), n
 560 = 10 saline-challenged pigs + diminazene aceturate (5 females, 5 males), n = 7 acid-challenged +
 561 diminazene aceturate pigs (4 females, 3 males). For panels C-F, n = 16 saline-challenged piglets

562 (8 females, 8 males), n = 16 acid-challenged pigs (8 females, 8 males), n = 10 saline-challenged
563 + diminazene aceturate (5 females, 5 males), n = 16 acid-challenged + diminazene aceturate pigs
564 (8 females, 8 males). Data points represent the mean fluorescent intensity for each piglet
565 calculated from 3-5 images analyzed (encompassing the anterior, middle and posterior regions of
566 the trachea). Abbreviations: DZ, diminazene aceturate; MUC5B, mucin 5B; MUC5AC, mucin
567 5AC. * $p < 0.05$ compared to saline-challenged pigs. Data were assessed with a parametric two-
568 way ANOVA followed by Sidak post hoc test. Mean \pm S.E.M shown.

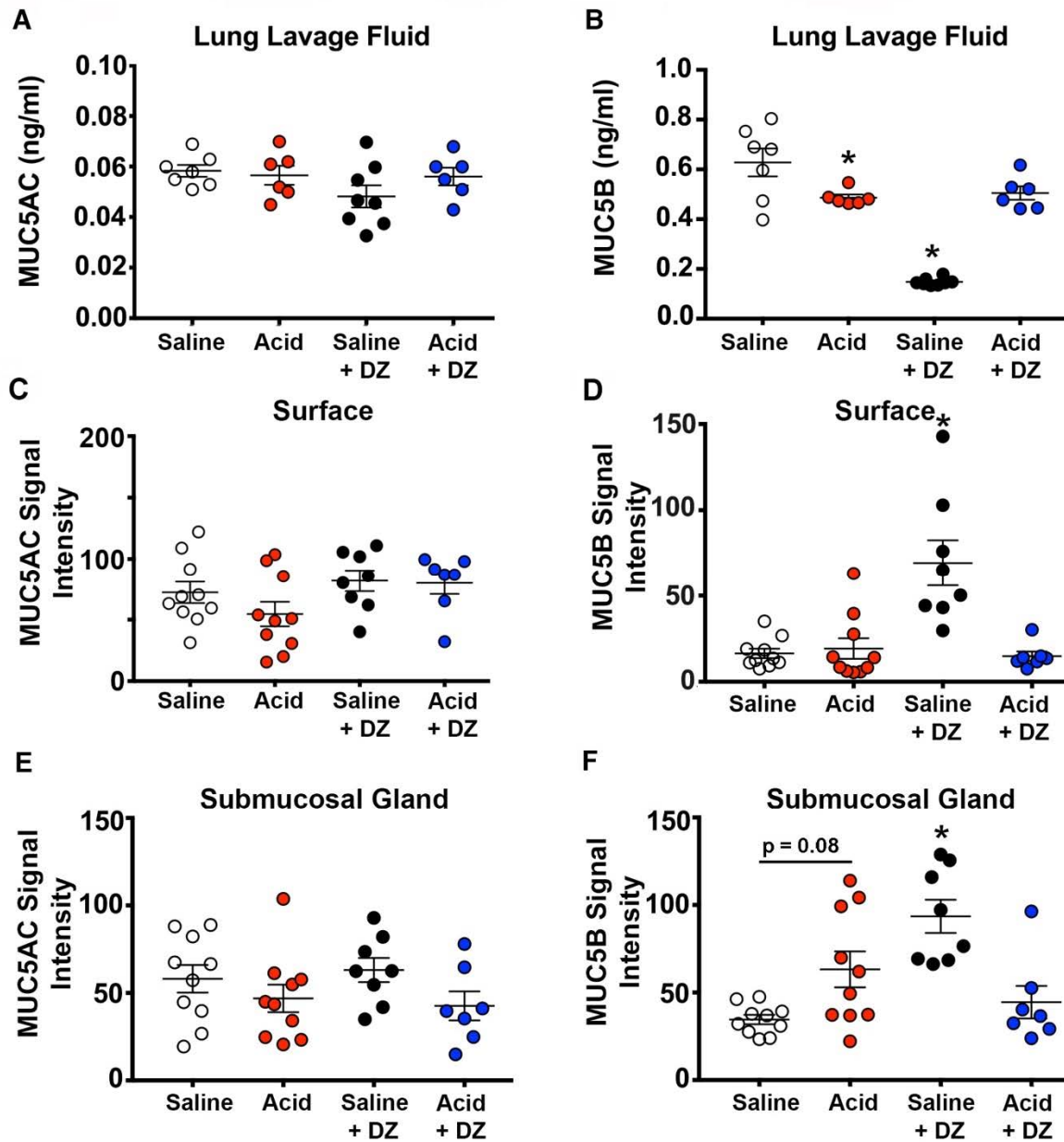
569

570

571

572

573



574

575 **Fig. 2. Mucin in piglet airways under methacholine-stimulated conditions.** Bronchoalveolar

576 lavage fluid concentrations of MU5AC (A) and MUC5B (B). MUC5AC and MUC5B staining

577 signal intensity of the surface epithelia (C, D) and submucosal gland (E, F). For panels A and B,

578 n = 7 saline-challenged piglets (4 females, 3 males), n = 6 acid-challenged pigs (3 females, 3

579 males), n = 8 saline-challenged + diminazene aceturate (4 females, 4 males), n = 6 acid-

580 challenged + diminazene aceturate pigs (3 females, 3 males). For panels C-F, n = 10 saline-

581 challenged piglets (5 females, 5 males), n = 10 acid-challenged pigs (5 females, 5 males), n = 8
582 saline-challenged + diminazene acetate (4 females, 4 males), n = 7 acid-challenged +
583 diminazene acetate pigs (4 females, 3 males). Data points represent the mean fluorescent
584 intensity for each piglet calculated from 3-5 images analyzed (encompassing the anterior, middle
585 and posterior regions of the trachea). Abbreviations: DZ, diminazene acetate; MUC5B, mucin
586 5B; MUC5AC, mucin 5AC. * $p < 0.05$ compared to saline-challenged pigs. Data were assessed
587 with a parametric two-way ANOVA followed by Sidak post hoc test. Mean \pm S.E.M shown.

588

589

590

591

592

600 males), n = 10 saline-challenged + diminazene aceturate (5 females, 5 males), n = 18 acid-
601 challenged + diminazene aceturate pigs (9 females, 9 males). Abbreviations: DZ, diminazene
602 aceturate. * p < 0.05 compared to saline-challenged pigs, # p < 0.05 compared to acid-challenged
603 piglets. Data were assessed with a non-parametric one-way ANOVA (Kruskal-Wallis) followed
604 by Dunn's multiple comparison test. Mean \pm S.E.M shown.

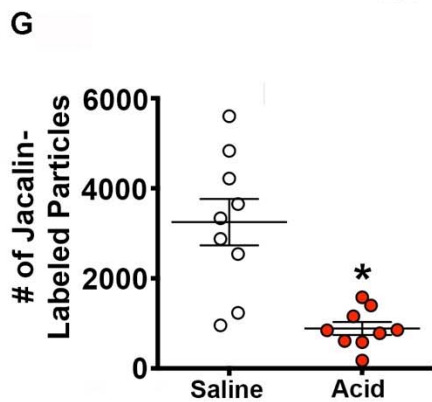
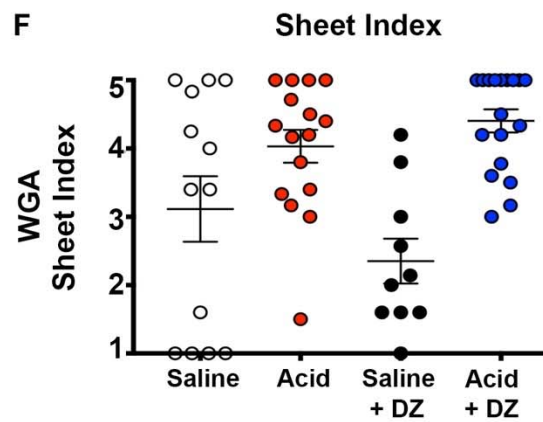
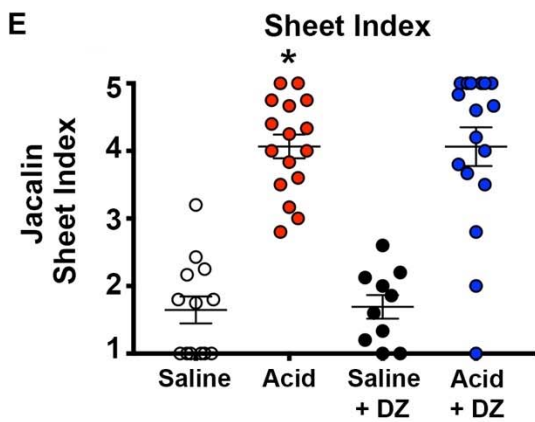
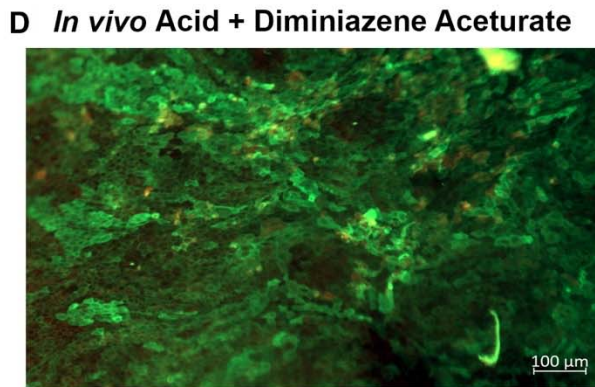
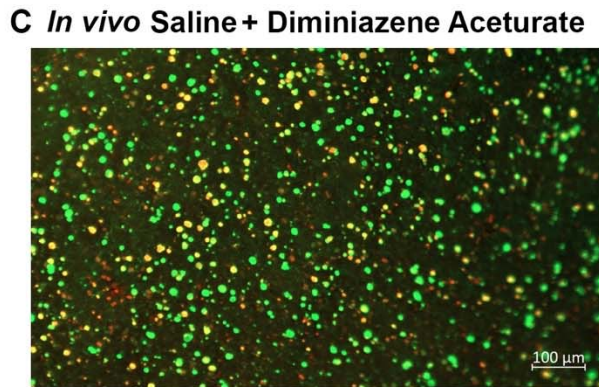
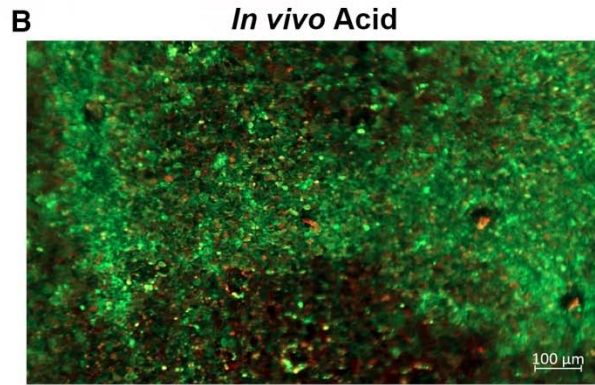
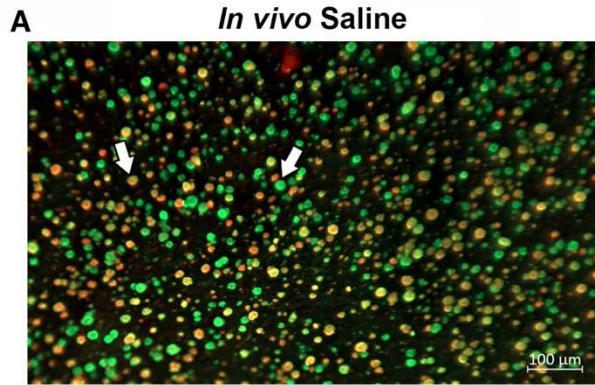
605

606

614 males), n = 10 acid-challenged pigs (4 females, 6 males), n = 8 saline-challenged + diminazene
615 aceturate (4 females, 4 males), n = 7 acid-challenged + diminazene aceturate pigs (4 females, 3
616 males). Abbreviations: DZ, diminazene aceturate. * p < 0.05 compared to saline-challenged pigs,
617 # p < 0.05 compared to acid-challenged piglets. Data were assessed with a non-parametric one-
618 way ANOVA (Kruskal-Wallis) followed by Dunn's multiple comparison test. Mean \pm S.E.M
619 shown.

620

621



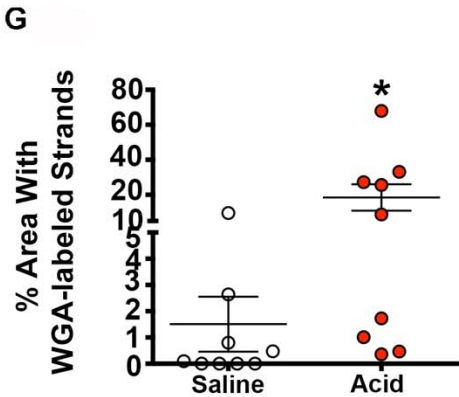
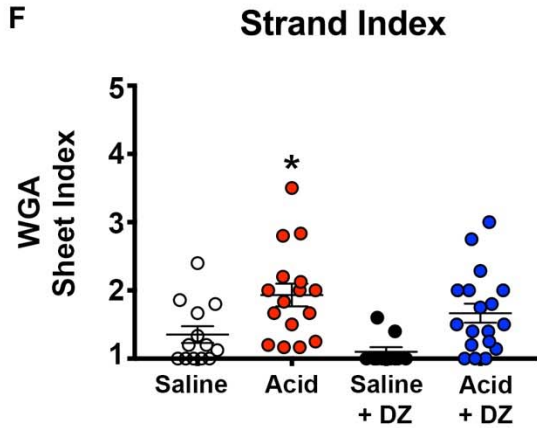
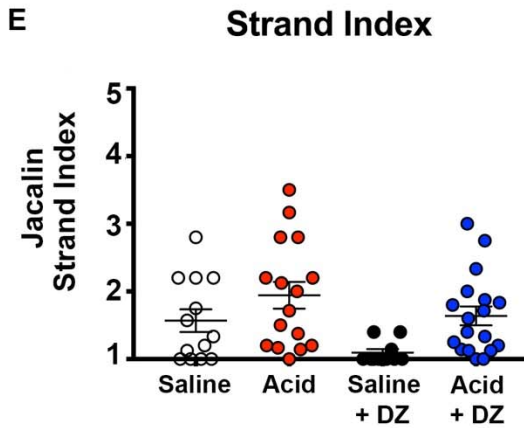
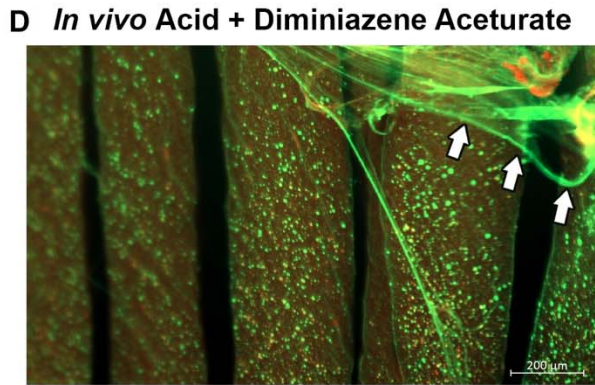
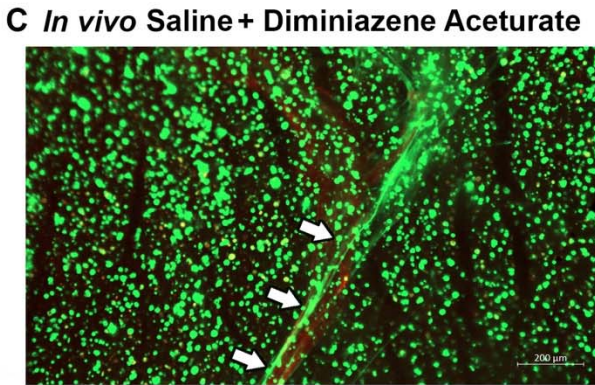
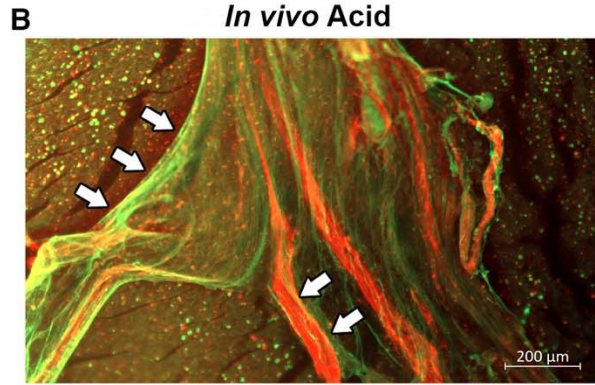
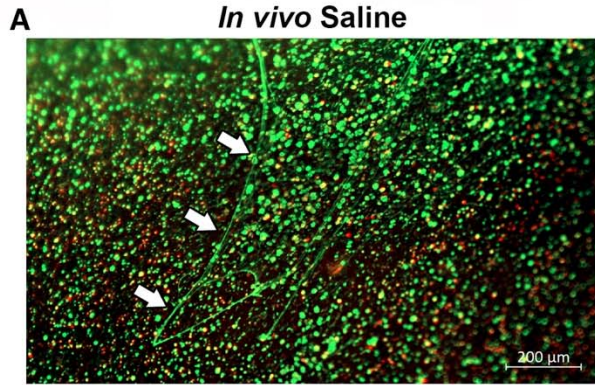
623 **Fig. 5. Mucus sheet formation under diminished bicarbonate and chloride transport. (A)**
624 Representative image of an *ex vivo* trachea from a saline-challenged piglet stimulated with
625 methacholine. Discrete entities of mucus were observed and visualized by jacalin lectin (green)
626 and wheat germ agglutinin lectin (red) staining. Arrows highlight examples of lectin labeling.
627 Representative images of methacholine-stimulated *ex vivo* tracheas from an acid-challenged
628 piglet (**B**), a saline-challenged + diminazene aceturate (**C**), and acid-challenged + diminazene
629 aceturate (**D**). Sheet index for jacalin-labeled mucus (**E**) and wheat germ agglutinin-labeled
630 mucus (**F**). (**G**) The numbers of jacalin-labeled mucus particles analyzed using IMARIS software
631 as an additional measurement of mucus sheet formation in acid-challenged piglets. n = 9 saline-
632 challenged piglets (4 females, 5 males), n = 9 acid-challenged pigs (4 females, 5 males). For
633 panels A-F, n = 13 saline-challenged piglets (7 females, 6 males), n = 16 acid-challenged pigs (8
634 females, 8 males), n = 10 saline-challenged + diminazene aceturate (5 females, 5 males), n = 18
635 acid-challenged + diminazene aceturate pigs (9 females, 9 males). Data points represent the
636 mean score for each piglet calculated from 5-7 analyzed images (encompassing the anterior,
637 middle and posterior regions of the trachea). Abbreviations: WGA, wheat germ agglutinin; DZ,
638 diminazene aceturate. * p < 0.05 compared to saline-challenged pigs. For panels E-F, data were
639 assessed with a non-parametric one-way ANOVA (Kruskal-Wallis) followed by Dunn's multiple
640 comparison test. For panel G, data were assessed by an unpaired students t-test. Mean \pm S.E.M
641 shown.

642

643

644

645



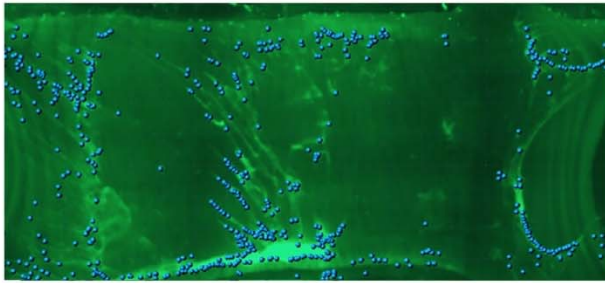
647 **Fig. 6. Mucus strand formation in acid-challenged piglets under diminished chloride and**
648 **bicarbonate transport conditions (A)** Representative image of an *ex vivo* trachea from a saline-
649 challenged piglet stimulated with methacholine. Mucus is labeled with jacalin lectin (green) and
650 wheat germ agglutinin lectin (red) staining. Arrows highlight an example of a mucus strand.
651 Representative images of *ex vivo* trachea from a saline-challenged (A), acid-challenged (B)
652 saline-challenged provided diminazene acetate (C), and acid-challenged pig provided
653 diminazene acetate (D) piglet airways stimulated with methacholine. Strand index for jacalin-
654 labeled mucus (E) and wheat germ agglutinin-labeled mucus (F). (G) The percent (%) of field of
655 view occupied by WGA-labeled strands. n = 9 saline-challenged piglets (4 females, 5 males), n =
656 9 acid-challenged pigs (4 females, 5 males). For panels A-F, n = 13 saline-challenged piglets (7
657 females, 6 males), n = 16 acid-challenged pigs (8 females, 8 males), n = 10 saline-challenged +
658 diminazene acetate (5 females, 5 males), n = 18 acid-challenged + diminazene acetate pigs (9
659 females, 9 males). Data points represent the mean score for each piglet calculated from 5-7
660 analyzed images (encompassing the anterior, middle and posterior regions of the trachea).
661 Abbreviations: WGA, wheat germ agglutinin; DZ, diminazene acetate. $p < 0.05$ compared to
662 saline-challenged pigs. For Panels E-F, data were assessed with a non-parametric one-way
663 ANOVA (Kruskal-Wallis) followed by Dunn's multiple comparison test. For panel G, data were
664 assessed by an unpaired students t-test. Mean \pm S.E.M shown.

665

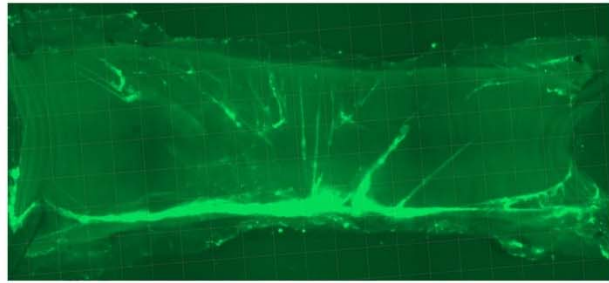
666

674 of a dilated duct openings with mucus emanating in acid-challenged piglets treated with
675 diminazene aceturate (**E**) Number of dilated submucosal gland ducts normalized to area. n =13
676 saline-challenged piglets (7 females, 6 males), n = 16 acid-challenged pigs (8 females, 8 males),
677 n = 10 saline-challenged + diminazene aceturate (5 females, 5 males), n = 18 acid-challenged +
678 diminazene aceturate pigs (9 females, 9 males). Data points represent the mean score for each
679 piglet calculated from 5-7 analyzed images (encompassing the anterior, middle and posterior
680 regions of the trachea). Abbreviations: DZ, diminazene aceturate. Data were assessed with a
681 parametric two-way ANOVA followed by Sidak post hoc test. Mean \pm S.E.M shown.

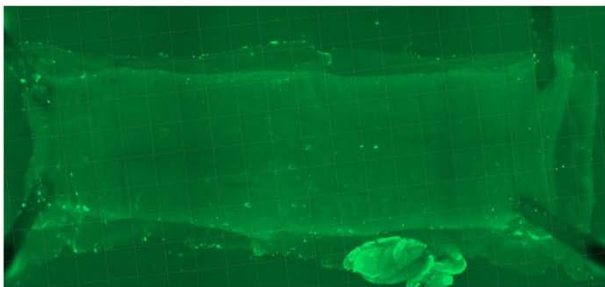
A IMARIS-Assisted Particle Assignment



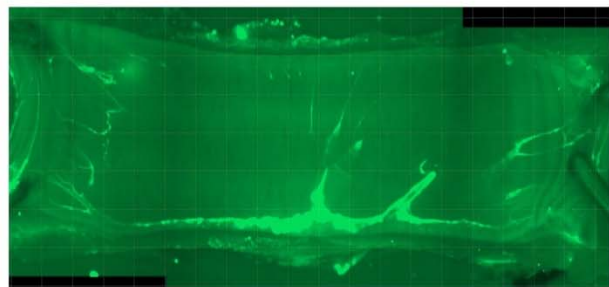
B *In vivo* Saline



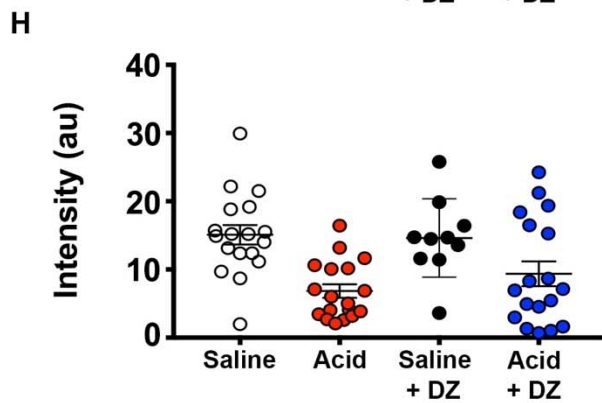
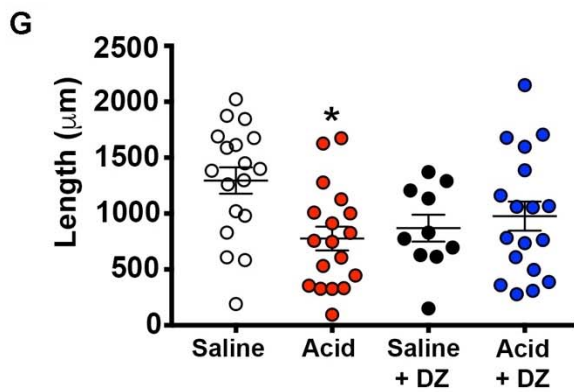
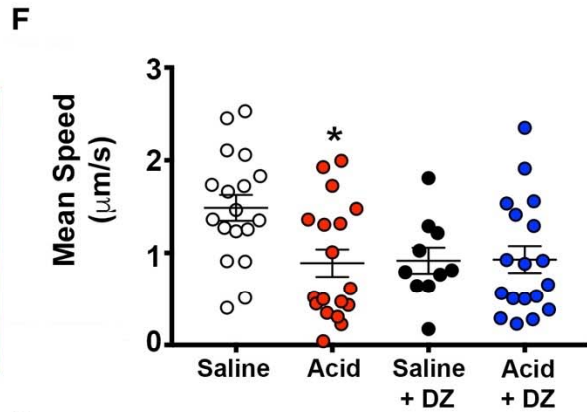
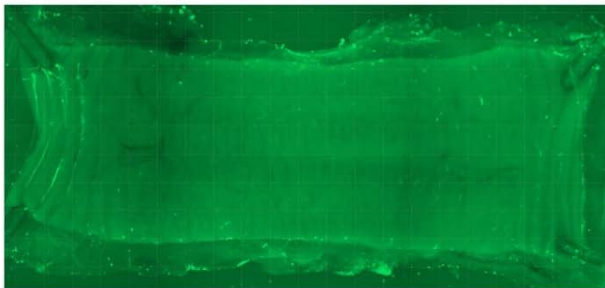
C *In vivo* Acid



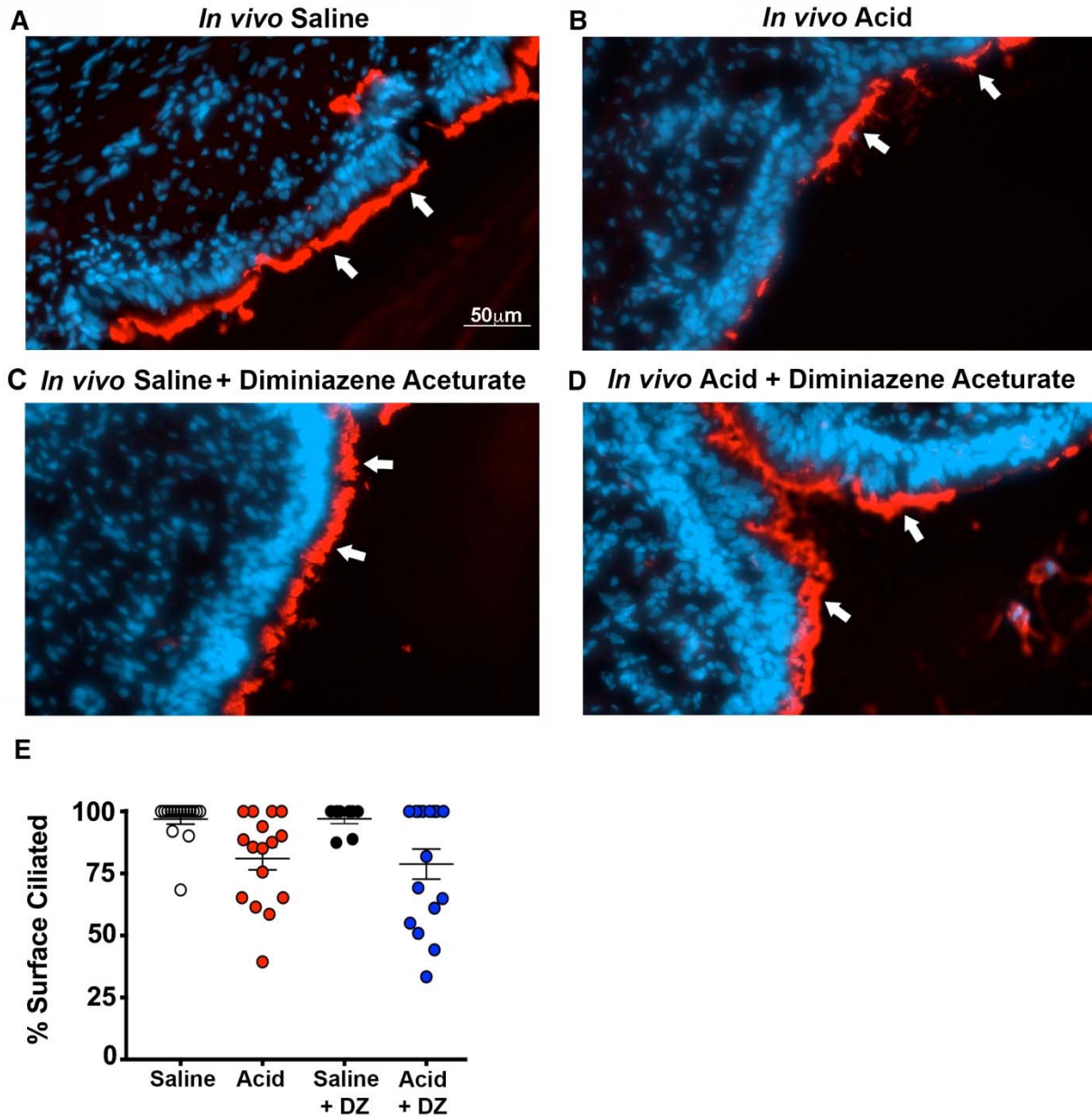
D *In Vivo* Saline + Diminiazene Aceturate



E *In Vivo* Acid + Diminiazene Aceturate



683 **Fig. 8. Mucus transport in piglet airways under diminished chloride and bicarbonate**
684 **transport. (A)** Representative image of an *ex vivo* piglet trachea stimulated with methacholine.
685 Mucus is visualized in real-time with fluorescent nanospheres (bright green). Mucus often forms
686 strands. Computer particles are assigned based upon fluorescence intensity and appear as
687 blue/aqua in color. Representative images of tracheas at the conclusion of the experiment post
688 methacholine stimulation in saline-challenged **(B)**, acid-challenge **(C)**, saline-challenged +
689 diminazene aceturate **(D)**, and acid-challenged + diminazene aceturate **(E)** piglet airways. **(F)**
690 Mean mucus transport speed. **(G)** Computer assigned particle-track length. **(H)** Quantification of
691 the signal intensity of fluorescently labeled mucus on the airway surface at the conclusion of the
692 experiment. n = 18 saline-challenged piglets (9 females, 9 males), n = 18 acid-challenged pigs (9
693 females, 9 males), n = 10 saline-challenged + diminazene aceturate (5 females, 5 males), n = 18
694 acid-challenged + diminazene aceturate pigs (9 females, 9 males). Abbreviations: DZ,
695 diminazene aceturate; au, arbitrary units. * $p < 0.05$ compared to saline-challenged pigs. Data
696 were assessed with a parametric two-way ANOVA followed by Sidak post hoc test. Mean \pm
697 S.E.M shown.
698



699
 700 **Fig. 9. Percent of trachea ciliated.** Representative images of cilia detected by antibody staining
 701 of acetylated tubulin (shown in red, highlighted by arrows) in tracheas from saline-challenged
 702 (A), acid-challenged (B), saline-challenged treated + diminazene aceturate (C), and acid-
 703 challenged + diminazene aceturate (D) piglets. (E) Quantification of ciliated trachea lumen
 704 expressed as a percentage (%) of the length of the epithelia that was ciliated divided by the total
 705 length of the epithelia. n = 16 saline-challenged piglets (8 females, 8 males), n = 16 acid-

706 challenged pigs (8 females, 8 males), n = 10 saline-challenged + diminazene aceturate (5
707 females, 5 males), n = 16 acid-challenged + diminazene aceturate pigs (8 females, 8 males).
708 Scale bar in panel A applies to panels B-D Abbreviations: DZ, diminazene aceturate. Data were
709 assessed with a parametric two-way ANOVA followed by Sidak post hoc test. Mean \pm S.E.M
710 shown.

711

712 **Acknowledgement**

713 We thank Dr. Dave Meyerholz and Dr. Mark Hoegger for helpful comments and suggestions.

714 The authors also thank Dr. Igancio Aguirre for providing technical support and resources.

715 **Funding:** This work was funded by R00HL119560, OT2OD026582 (PI, LRR) and

716 OT2OD023854 (Co-I, LRR). **Author contributions:** L.R.R, YS.J.L, SP.K, M.V.G, E.N.C and

717 L.B, E.E, M.S, K.R.A participated in the conception and design of the research. L.R.R, SP.K,

718 YS.J.L, J.S.D, E.N.C, M.V.G, V.S, L.B, E.E, M.S, and K.V performed the experiments. L.R.R,

719 SP.K, YS.J.L, E.N.C, M.V.G, L.B, and K.R.A analyzed the data. L.R.R, YS.J.L, SP.K, J.S.D,

720 E.N.C, M.V.G, K.R.A interpreted the results of the experiments. L.R.R and K.R.A prepared the

721 figures. L.R.R and M.V.G. drafted the manuscript. All authors edited and reviewed the

722 manuscript. **Competing interests:** The authors declare no competing interests. **Data and**

723 **materials availability:** All data is available in the manuscript.

724

725 **REFERENCES AND NOTES**

726 1. Appendix 1 BSA Conversion Charts. 286-289.

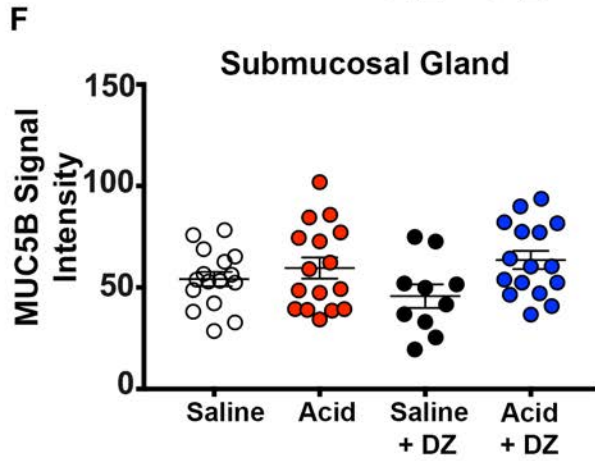
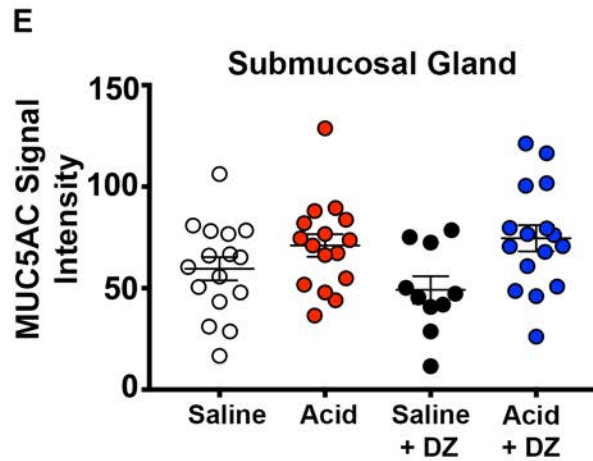
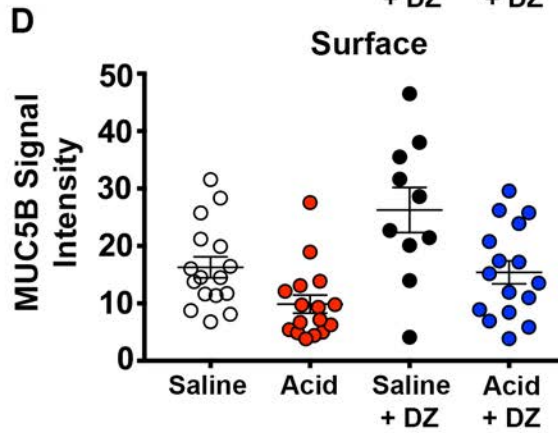
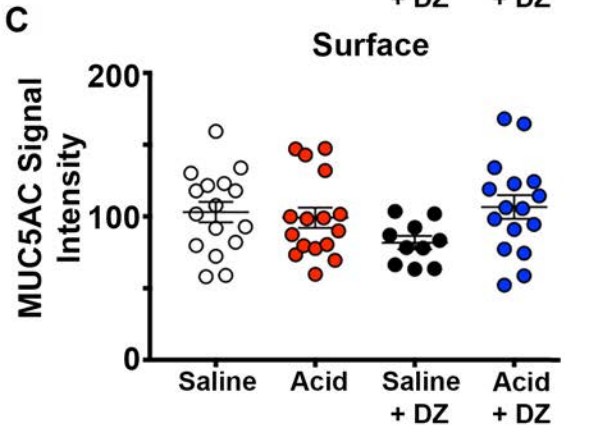
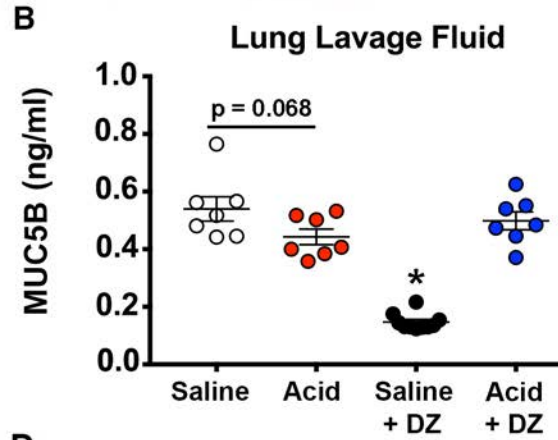
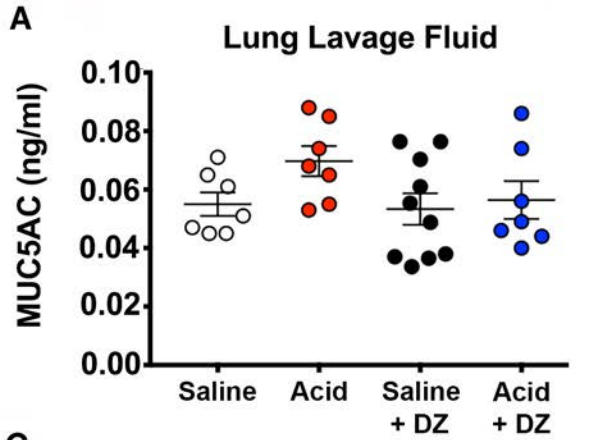
727 2. **Abdullah LH, Coakley R, Webster MJ, Zhu Y, Tarran R, Radicioni G, Kesimer M,**
728 **Boucher RC, Davis CW, and Ribeiro CMP.** Mucin Production and Hydration Responses to
729 Mucopurulent Materials in Normal versus Cystic Fibrosis Airway Epithelia. *Am J Respir Crit*
730 *Care Med* 197: 481-491, 2018.

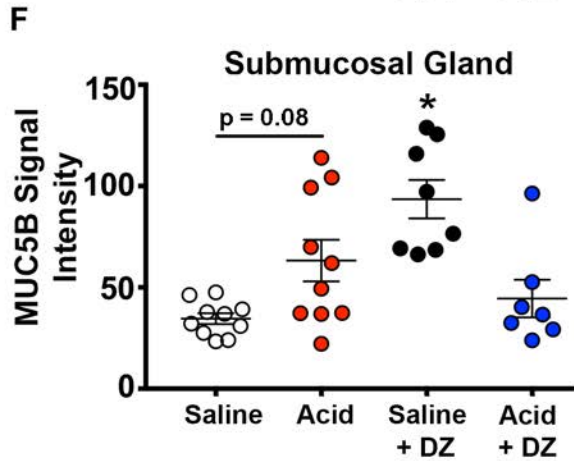
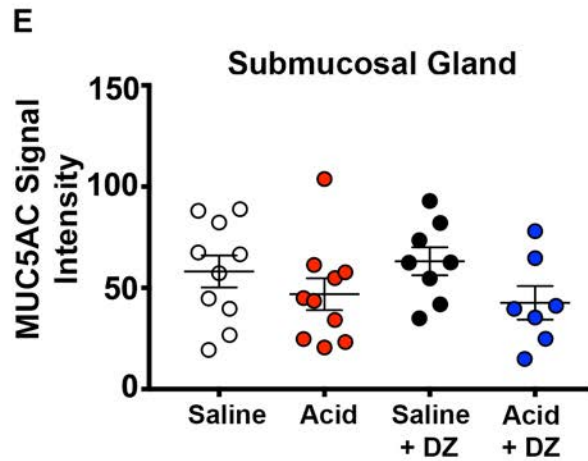
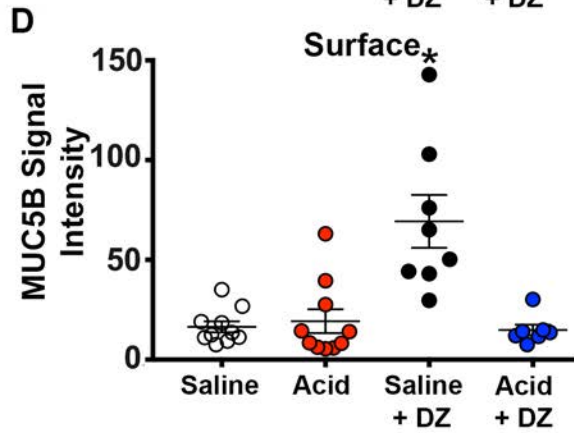
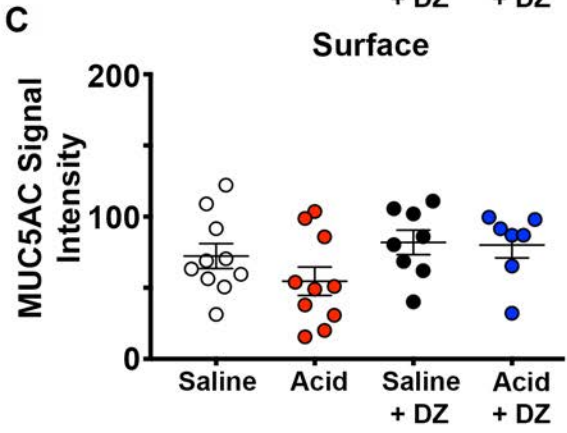
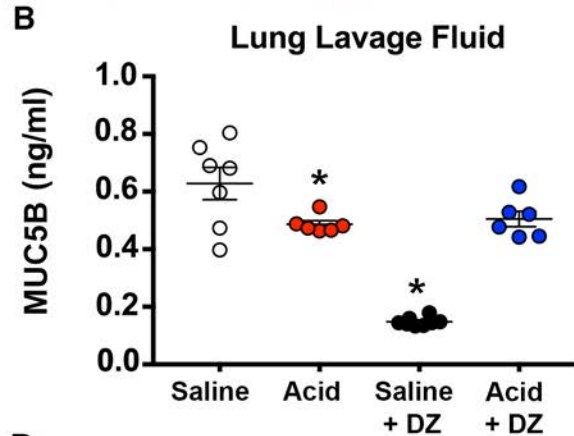
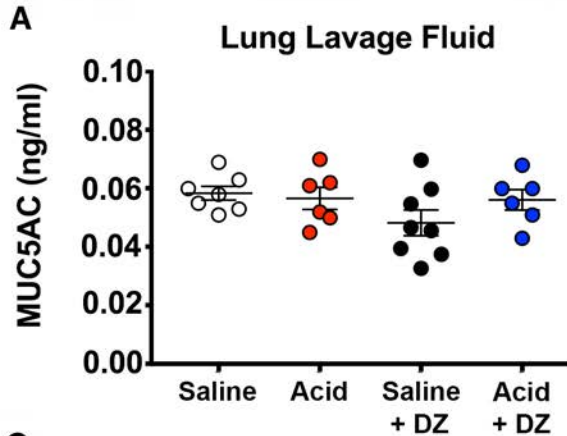
- 731 3. **Abdullah LH, Wolber C, Kesimer M, Sheehan JK, and Davis CW.** Studying mucin
732 secretion from human bronchial epithelial cell primary cultures. *Methods Mol Biol* 842: 259-277,
733 2012.
- 734 4. **Abou Alaiwa MH, Beer AM, Pezzulo AA, Launspach JL, Horan RA, Stoltz DA,**
735 **Starner TD, Welsh MJ, and Zabner J.** Neonates with cystic fibrosis have a reduced nasal
736 liquid pH; a small pilot study. *J Cyst Fibros* 13: 373-377, 2014.
- 737 5. **Birket SE, Davis JM, Fernandez CM, Tuggle KL, Oden AM, Chu KK, Tearney GJ,**
738 **Fanucchi MV, Sorscher EJ, and Rowe SM.** Development of an airway mucus defect in the
739 cystic fibrosis rat. *JCI Insight* 3: 2018.
- 740 6. **Burgel PR, Montani D, Danel C, Dusser DJ, and Nadel JA.** A morphometric study of
741 mucins and small airway plugging in cystic fibrosis. *Thorax* 62: 153-161, 2007.
- 742 7. **Button B, Cai LH, Ehre C, Kesimer M, Hill DB, Sheehan JK, Boucher RC, and**
743 **Rubinstein M.** A periciliary brush promotes the lung health by separating the mucus layer from
744 airway epithelia. *Science* 337: 937-941, 2012.
- 745 8. **Castardeli C, Sartorio CL, Pimentel EB, Forechi L, and Mill JG.** The ACE 2
746 activator diminazene aceturate (DIZE) improves left ventricular diastolic dysfunction following
747 myocardial infarction in rats. *Biomed Pharmacother* 107: 212-218, 2018.
- 748 9. **Chen G, Sun L, Kato T, Okuda K, Martino MB, Abzhanova A, Lin JM, Gilmore**
749 **RC, Batson BD, O'Neal YK, Volmer AS, Dang H, Deng Y, Randell SH, Button B, Livraghi-**
750 **Butrico A, Kesimer M, Ribeiro CM, O'Neal WK, and Boucher RC.** IL-1beta dominates the
751 promucin secretory cytokine profile in cystic fibrosis. *J Clin Invest* 2019.
- 752 10. **Chen X, Qiu L, Li M, Durrnagel S, Orser BA, Xiong ZG, and MacDonald JF.**
753 Diarylamidines: high potency inhibitors of acid-sensing ion channels. *Neuropharmacology* 58:
754 1045-1053, 2010.
- 755 11. **Cooney AL, Abou Alaiwa MH, Shah VS, Bouzek DC, Stroik MR, Powers LS,**
756 **Gansemer ND, Meyerholz DK, Welsh MJ, Stoltz DA, Sinn PL, and McCray PB, Jr.**
757 Lentiviral-mediated phenotypic correction of cystic fibrosis pigs. *JCI Insight* 1: 2016.
- 758 12. **Cooney AL, Singh BK, Loza LM, Thornell IM, Hippee CE, Powers LS, Ostedgaard**
759 **LS, Meyerholz DK, Wohlford-Lenane C, Stoltz DA, B. McCray P J, and Sinn PL.**
760 Widespread airway distribution and short-term phenotypic correction of cystic fibrosis pigs
761 following aerosol delivery of piggyBac/adenovirus. *Nucleic Acids Res* 46: 9591-9600, 2018.
- 762 13. **Elamin EA, Homeida AM, Adam SE, and Mahmoud MM.** The efficacy of berenil
763 (diminazene aceturate) against *Trypanosoma evansi* infection in mice. *Journal of veterinary*
764 *pharmacology and therapeutics* 5: 259-265, 1982.
- 765 14. **Ermund A, Meiss LN, Dolan B, Bahr A, Klymiuk N, and Hansson GC.** The mucus
766 bundles responsible for airway cleaning are retained in cystic fibrosis and by cholinergic
767 stimulation. *Eur Respir J* 52: 2018.
- 768 15. **Esther CR, Jr., Muhlebach MS, Ehre C, Hill DB, Wolfgang MC, Kesimer M,**
769 **Ramsey KA, Markovetz MR, Garbarine IC, Forest MG, Seim I, Zorn B, Morrison CB,**
770 **Delion MF, Thelin WR, Villalon D, Sabater JR, Turkovic L, Ranganathan S, Stick SM, and**
771 **Boucher RC.** Mucus accumulation in the lungs precedes structural changes and infection in
772 children with cystic fibrosis. *Sci Transl Med* 11: 2019.
- 773 16. **Foundation CF.** Cystic Fibrosis Foundation. online: 2016.
- 774 17. **Gilbert RJ.** Studies in rabbits on the disposition and trypanocidal activity of the anti-
775 trypanosomal drug, diminazene aceturate (Berenil). *Br J Pharmacol* 80: 133-139, 1983.

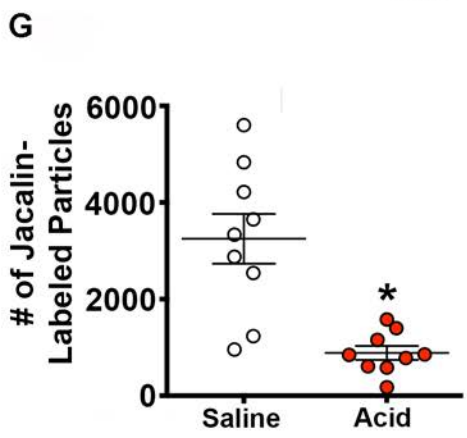
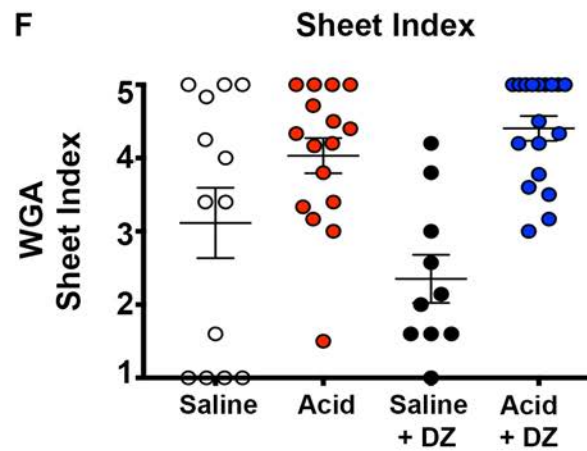
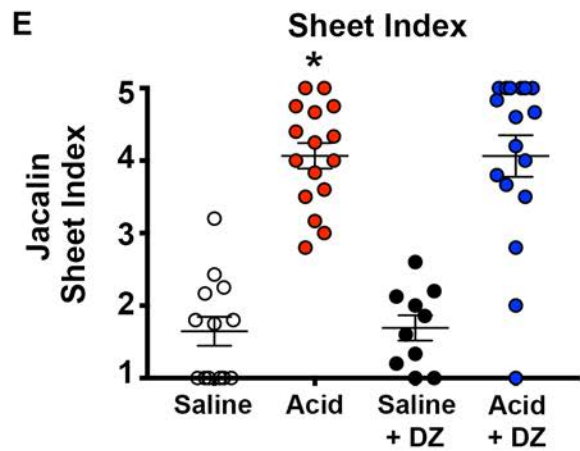
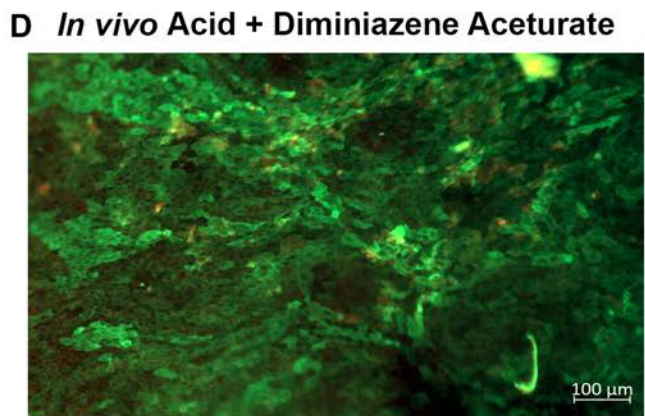
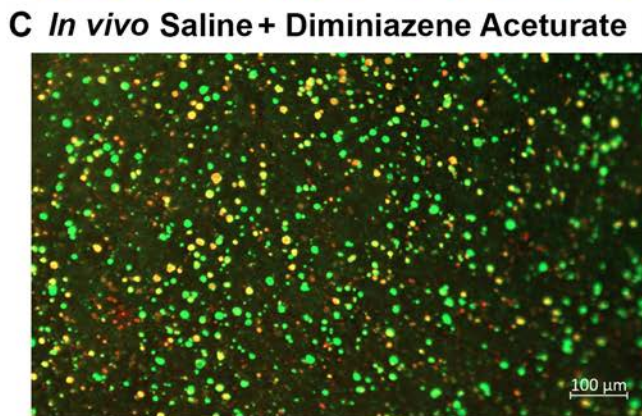
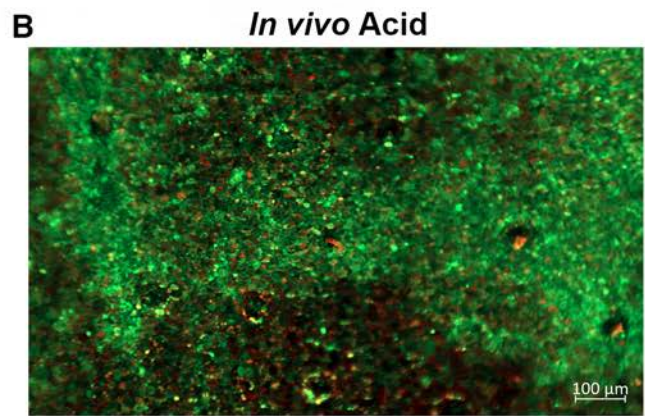
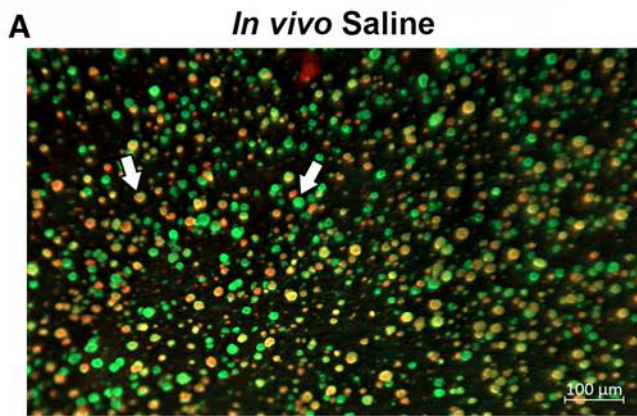
- 776 18. **Gu Q, and Lee LY.** Characterization of acid signaling in rat vagal pulmonary sensory
777 neurons. *Am J Physiol Lung Cell Mol Physiol* 291: L58-65, 2006.
- 778 19. **Henderson AG, Ehre C, Button B, Abdullah LH, Cai LH, Leigh MW, DeMaria GC,**
779 **Matsui H, Donaldson SH, Davis CW, Sheehan JK, Boucher RC, and Kesimer M.** Cystic
780 fibrosis airway secretions exhibit mucin hyperconcentration and increased osmotic pressure. *J*
781 *Clin Invest* 124: 3047-3060, 2014.
- 782 20. **Henke MO, John G, Germann M, Lindemann H, and Rubin BK.** MUC5AC and
783 MUC5B mucins increase in cystic fibrosis airway secretions during pulmonary exacerbation. *Am*
784 *J Respir Crit Care Med* 175: 816-821, 2007.
- 785 21. **Hill DB, Long RF, Kissner WJ, Atieh E, Garbarine IC, Markovetz MR, Fontana**
786 **NC, Christy M, Habibpour M, Tarran R, Forest MG, Boucher RC, and Button B.**
787 Pathological mucus and impaired mucus clearance in cystic fibrosis patients result from
788 increased concentration, not altered pH. *Eur Respir J* 52: 2018.
- 789 22. **Hoegger MJ, Fischer AJ, McMenimen JD, Ostedgaard LS, Tucker AJ, Awadalla**
790 **MA, Moninger TO, Michalski AS, Hoffman EA, Zabner J, Stoltz DA, and Welsh MJ.**
791 Impaired mucus detachment disrupts mucociliary transport in a piglet model of cystic fibrosis.
792 *Science* 345: 818-822, 2014.
- 793 23. **Hughes GW, Ridley C, Collins R, Roseman A, Ford R, and Thornton DJ.** The
794 MUC5B mucin polymer is dominated by repeating structural motifs and its topology is regulated
795 by calcium and pH. *Sci Rep* 9: 17350, 2019.
- 796 24. **Jaqaman K, Loerke D, Mettlen M, Kuwata H, Grinstein S, Schmid SL, and Danuser**
797 **G.** Robust single-particle tracking in live-cell time-lapse sequences. *Nat Methods* 5: 695-702,
798 2008.
- 799 25. **Knowles MR, and Boucher RC.** Mucus clearance as a primary innate defense
800 mechanism for mammalian airways. *J Clin Invest* 109: 571-577, 2002.
- 801 26. **Kollarik M, and Udem BJ.** Mechanisms of acid-induced activation of airway afferent
802 nerve fibres in guinea-pig. *J Physiol* 543: 591-600, 2002.
- 803 27. **Kreda SM, Davis CW, and Rose MC.** CFTR, mucins, and mucus obstruction in cystic
804 fibrosis. *Cold Spring Harb Perspect Med* 2: a009589, 2012.
- 805 28. **Kuan SP, Liao YJ, Davis KM, Messer JG, Zubcevic J, Aguirre JI, and Reznikov**
806 **LR.** Attenuated Amiloride-Sensitive Current and Augmented Calcium-Activated Chloride
807 Current in Marsh Rice Rat (*Oryzomys palustris*) Airways. *iScience* 19: 737-748, 2019.
- 808 29. **Lee JYP, Saez NJ, Cristofori-Armstrong B, Anangi R, King GF, Smith MT, and**
809 **Rash LD.** Inhibition of acid-sensing ion channels by diminazene and APETx2 evoke partial and
810 highly variable antihyperalgesia in a rat model of inflammatory pain. *Br J Pharmacol* 175: 2204-
811 2218, 2018.
- 812 30. **Lee LY, Gu Q, Xu F, and Hong JL.** Acid-sensing by airway afferent nerves. *Pulm*
813 *Pharmacol Ther* 26: 491-497, 2013.
- 814 31. **MacLean DM, and Jayaraman V.** Deactivation kinetics of acid-sensing ion channel 1a
815 are strongly pH-sensitive. *Proc Natl Acad Sci U S A* 114: E2504-E2513, 2017.
- 816 32. **Mall M, Grubb BR, Harkema JR, O'Neal WK, and Boucher RC.** Increased airway
817 epithelial Na⁺ absorption produces cystic fibrosis-like lung disease in mice. *Nat Med* 10: 487-
818 493, 2004.
- 819 33. **McShane D, Davies JC, Davies MG, Bush A, Geddes DM, and Alton EW.** Airway
820 surface pH in subjects with cystic fibrosis. *Eur Respir J* 21: 37-42, 2003.

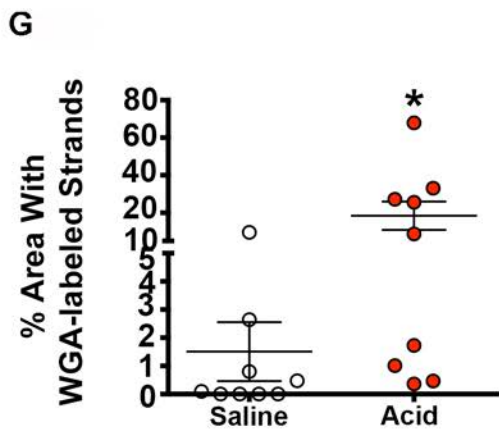
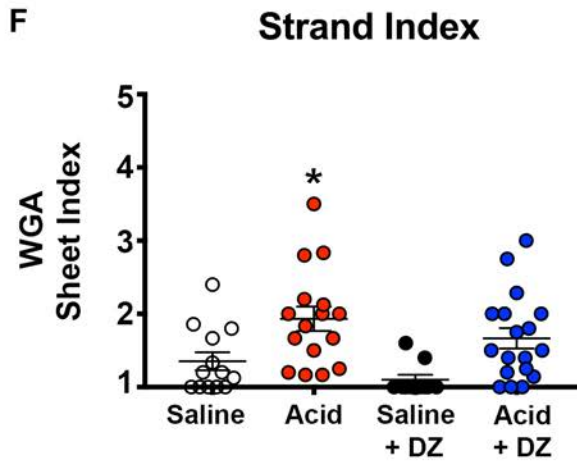
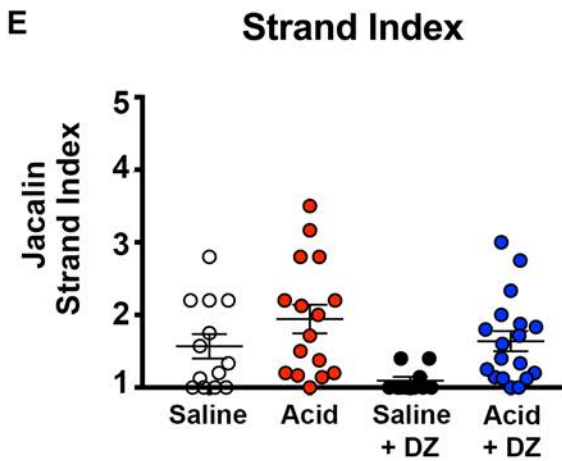
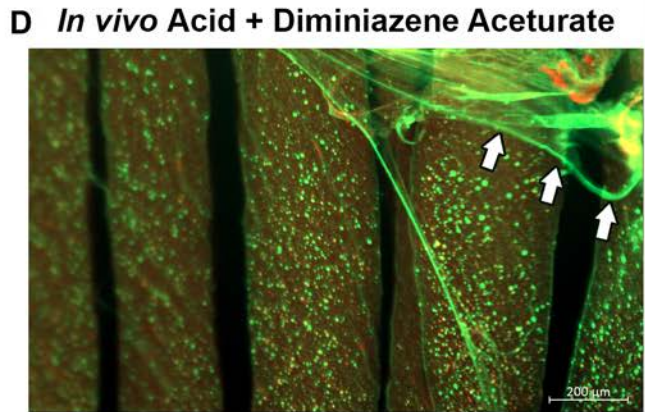
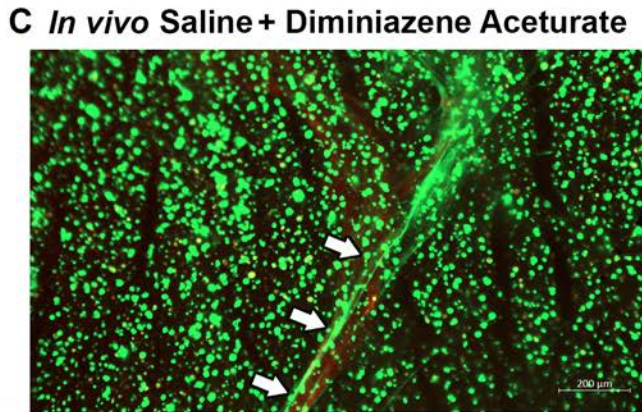
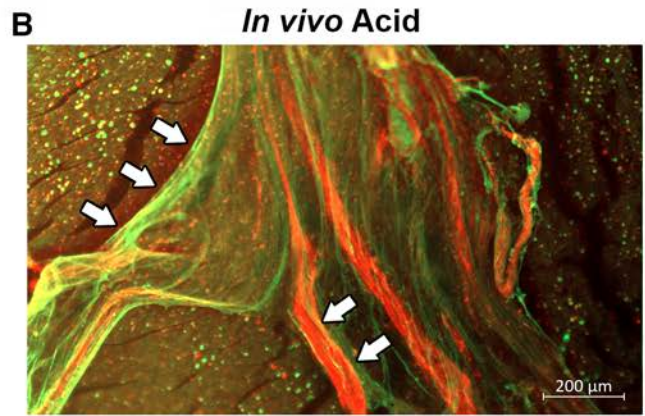
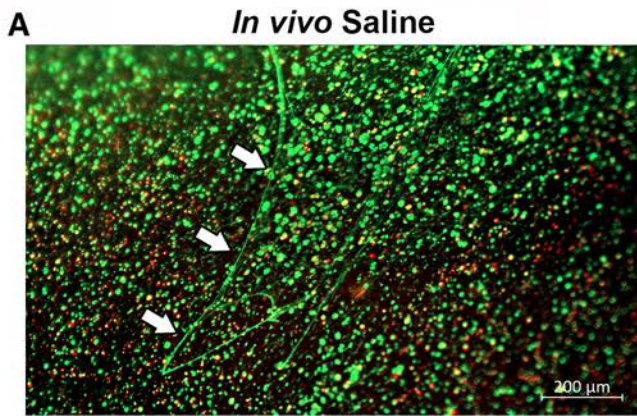
- 821 34. **Newhouse MT, Rossman CM, Dolovich J, Dolovich MB, and Wilson WM.**
822 Impairment of mucociliary transport in cystic fibrosis. *Mod Probl Paediatr* 19: 190-198, 1976.
- 823 35. **Onyeyili PA, and Anika SM.** Diminazene aceturate residues in the tissues of healthy,
824 *Trypanosoma congolense* and *Trypanosoma brucei brucei* infected dogs. *Br Vet J* 147: 155-162,
825 1991.
- 826 36. **Ostedgaard LS, Moninger TO, McMenimen JD, Sawin NM, Parker CP, Thornell**
827 **IM, Powers LS, Gansemer ND, Bouzek DC, Cook DP, Meyerholz DK, Abou Alaiwa MH,**
828 **Stoltz DA, and Welsh MJ.** Gel-forming mucins form distinct morphologic structures in
829 airways. *Proc Natl Acad Sci U S A* 114: 6842-6847, 2017.
- 830 37. **Park JA, and Fredberg JJ.** Cell Jamming in the Airway Epithelium. *Ann Am Thorac*
831 *Soc* 13 Suppl 1: S64-67, 2016.
- 832 38. **Pezzulo AA, Tang XX, Hoegger MJ, Alaiwa MH, Ramachandran S, Moninger TO,**
833 **Karp PH, Wohlford-Lenane CL, Haagsman HP, van Eijk M, Banfi B, Horswill AR, Stoltz**
834 **DA, McCray PB, Jr., Welsh MJ, and Zabner J.** Reduced airway surface pH impairs bacterial
835 killing in the porcine cystic fibrosis lung. *Nature* 487: 109-113, 2012.
- 836 39. **Price MP, Gong H, Parsons MG, Kundert JR, Reznikov LR, Bernardinelli L,**
837 **Chaloner K, Buchanan GF, Wemmie JA, Richerson GB, Cassell MD, and Welsh MJ.**
838 Localization and behaviors in null mice suggest that ASIC1 and ASIC2 modulate responses to
839 aversive stimuli. *Genes Brain Behav* 13: 179-194, 2014.
- 840 40. **Quinton PM.** Cystic fibrosis: impaired bicarbonate secretion and mucoviscidosis. *Lancet*
841 372: 415-417, 2008.
- 842 41. **Quinton PM.** Role of epithelial HCO₃⁻ transport in mucin secretion: lessons from
843 cystic fibrosis. *Am J Physiol Cell Physiol* 299: C1222-1233, 2010.
- 844 42. **Rajapaksha IG, Mak KY, Huang P, Burrell LM, Angus PW, and Herath CB.** The
845 small molecule drug diminazene aceturate inhibits liver injury and biliary fibrosis in mice. *Sci*
846 *Rep* 8: 10175, 2018.
- 847 43. **Ramsey BW, Banks-Schlegel S, Accurso FJ, Boucher RC, Cutting GR, Engelhardt**
848 **JF, Guggino WB, Karp CL, Knowles MR, Kolls JK, LiPuma JJ, Lynch S, McCray PB, Jr.,**
849 **Rubenstein RC, Singh PK, Sorscher E, and Welsh M.** Future directions in early cystic fibrosis
850 lung disease research: an NHLBI workshop report. *Am J Respir Crit Care Med* 185: 887-892,
851 2012.
- 852 44. **Reddi BA.** Why is saline so acidic (and does it really matter?). *Int J Med Sci* 10: 747-
853 750, 2013.
- 854 45. **Reznikov LR, Liao YSJ, Gu T, Davis KM, Kuan SP, Atanasova KR, Dadural JS,**
855 **Collins EN, Guevara MV, and Vogt K.** Sex-specific airway hyperreactivity and sex-specific
856 transcriptome remodeling in neonatal piglets challenged with intra-airway acid. *Am J Physiol*
857 *Lung Cell Mol Physiol* 316: L131-L143, 2019.
- 858 46. **Reznikov LR, Meyerholz DK, Abou Alaiwa M, Kuan SP, Liao YJ, Bormann NL,**
859 **Bair TB, Price M, Stoltz DA, and Welsh MJ.** The vagal ganglia transcriptome identifies
860 candidate therapeutics for airway hyperreactivity. *Am J Physiol Lung Cell Mol Physiol* 315:
861 L133-L148, 2018.
- 862 47. **Reznikov LR, Meyerholz DK, Adam RJ, Abou Alaiwa M, Jaffer O, Michalski AS,**
863 **Powers LS, Price MP, Stoltz DA, and Welsh MJ.** Acid-Sensing Ion Channel 1a Contributes to
864 Airway Hyperreactivity in Mice. *PLoS One* 11: e0166089, 2016.

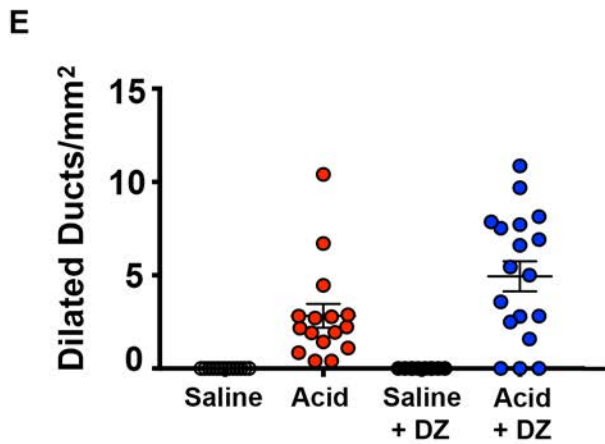
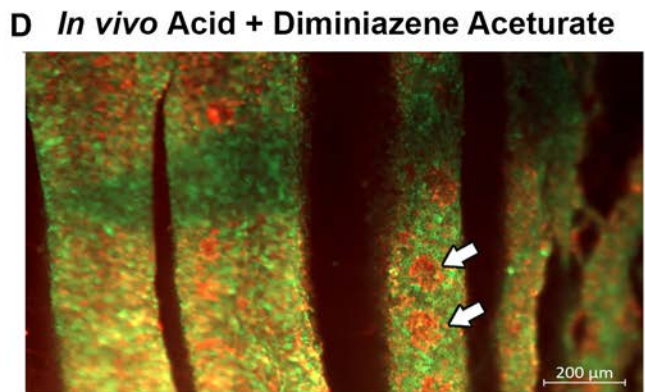
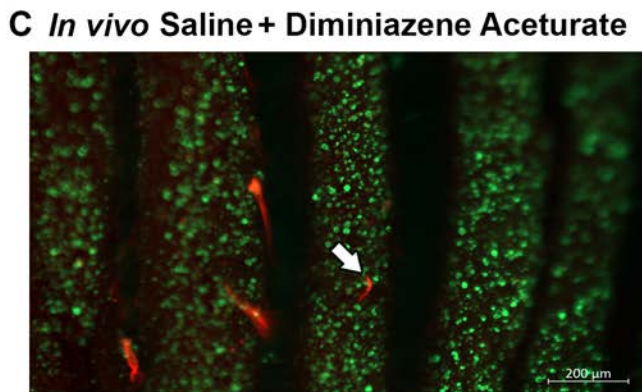
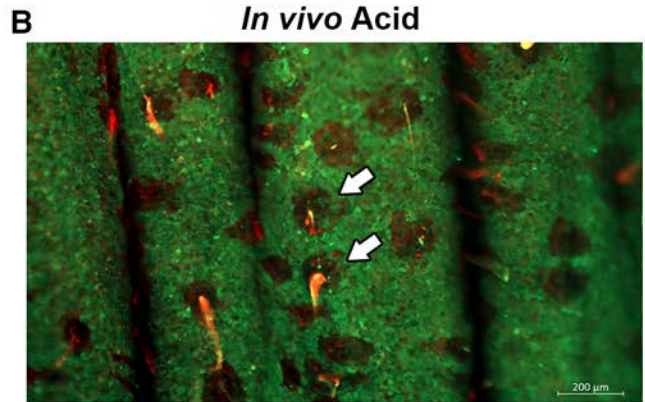
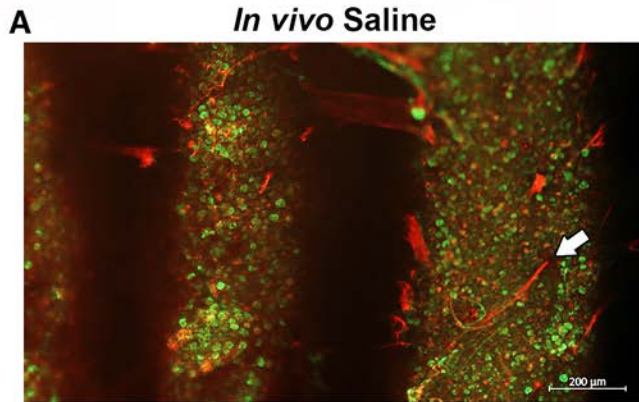
- 865 48. **Reznikov LR, Meyerholz DK, Kuan SP, Guevara MV, Atanasova KR, and Abou**
866 **Alaiwa MH.** Solitary Cholinergic Stimulation Induces Airway Hyperreactivity and Transcription
867 of Distinct Pro-inflammatory Pathways. *Lung* 196: 219-229, 2018.
- 868 49. **Ridley C, Kouvatso N, Raynal BD, Howard M, Collins RF, Desseyn JL, Jowitt TA,**
869 **Baldock C, Davis CW, Hardingham TE, and Thornton DJ.** Assembly of the respiratory
870 mucin MUC5B: a new model for a gel-forming mucin. *J Biol Chem* 289: 16409-16420, 2014.
- 871 50. **Rosen BH, Evans TIA, Moll SR, Gray JS, Liang B, Sun X, Zhang Y, Jensen-Cody**
872 **CW, Swatek AM, Zhou W, He N, Rotti PG, Tyler SR, Keiser NW, Anderson PJ, Brooks L,**
873 **Li Y, Pope RM, Rajput M, Hoffman EA, Wang K, Harris JK, Parekh KR, Gibson-Corley**
874 **KN, and Engelhardt JF.** Infection Is Not Required for Muco-inflammatory Lung Disease in
875 CFTR-Knockout Ferrets. *Am J Respir Crit Care Med* 197: 1308-1318, 2018.
- 876 51. **Rosenfeld M, Emerson J, Williams-Warren J, Pepe M, Smith A, Montgomery AB,**
877 **and Ramsey B.** Defining a pulmonary exacerbation in cystic fibrosis. *J Pediatr* 139: 359-365,
878 2001.
- 879 52. **Salinas D, Haggie PM, Thiagarajah JR, Song Y, Rosbe K, Finkbeiner WE, Nielson**
880 **DW, and Verkman AS.** Submucosal gland dysfunction as a primary defect in cystic fibrosis.
881 *FASEB J* 19: 431-433, 2005.
- 882 53. **Schmidt A, Rossetti G, Jousen S, and Grunder S.** Diminazene Is a Slow Pore Blocker
883 of Acid-Sensing Ion Channel 1a (ASIC1a). *Mol Pharmacol* 92: 665-675, 2017.
- 884 54. **Schultz A, Puvvadi R, Borisov SM, Shaw NC, Klimant I, Berry LJ, Montgomery**
885 **ST, Nguyen T, Kreda SM, Kicic A, Noble PB, Button B, and Stick SM.** Airway surface liquid
886 pH is not acidic in children with cystic fibrosis. *Nat Commun* 8: 1409, 2017.
- 887 55. **Sisson JH, Papi A, Beckmann JD, Leise KL, Wisecarver J, Brodersen BW, Kelling**
888 **CL, Spurzem JR, and Rennard SI.** Smoke and viral infection cause cilia loss detectable by
889 bronchoalveolar lavage cytology and dynein ELISA. *Am J Respir Crit Care Med* 149: 205-213,
890 1994.
- 891 56. **Sutto Z, Conner GE, and Salathe M.** Regulation of human airway ciliary beat
892 frequency by intracellular pH. *J Physiol* 560: 519-532, 2004.
- 893 57. **Talbot S, Doyle B, Huang J, Wang JC, Ahmadi M, Roberson DP, Yekkirala A,**
894 **Foster SL, Browne LE, Bean BP, Levy BD, and Woolf CJ.** Vagal sensory neurons drive
895 mucous cell metaplasia. *J Allergy Clin Immunol* 2020.
- 896 58. **Tang XX, Ostedgaard LS, Hoegger MJ, Moninger TO, Karp PH, McMenimen JD,**
897 **Choudhury B, Varki A, Stoltz DA, and Welsh MJ.** Acidic pH increases airway surface liquid
898 viscosity in cystic fibrosis. *J Clin Invest* 126: 879-891, 2016.
- 899 59. **Wang R, and Ware JH.** Detecting moderator effects using subgroup analyses. *Prev Sci*
900 14: 111-120, 2013.
- 901 60. **Wong CH, Matai R, and Morice AH.** Cough induced by low pH. *Respir Med* 93: 58-
902 61, 1999.
- 903 61. **Zuelzer WW, and Newton WA, Jr.** The pathogenesis of fibrocystic disease of the
904 pancreas; a study of 36 cases with special reference to the pulmonary lesions. *Pediatrics* 4: 53-
905 69, 1949.
- 906



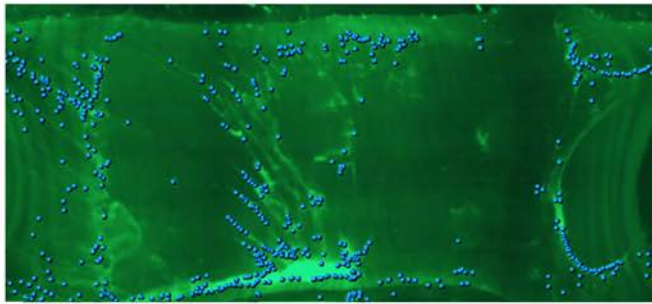




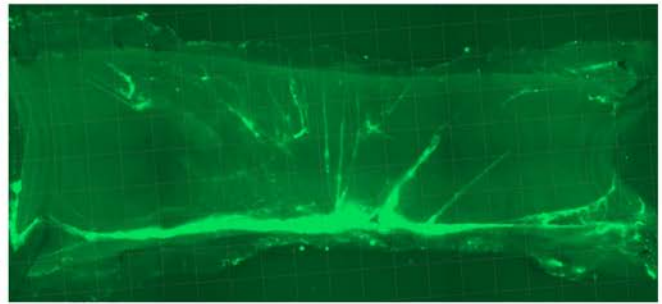




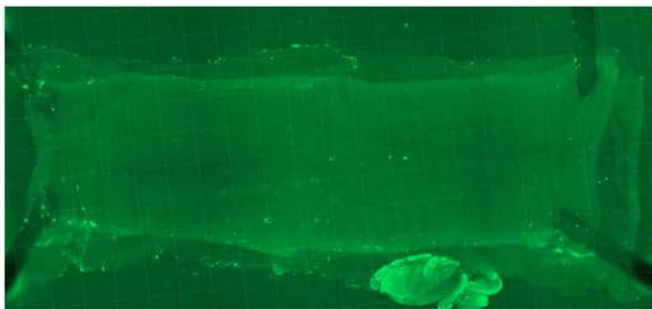
A IMARIS-Assisted Particle Assignment



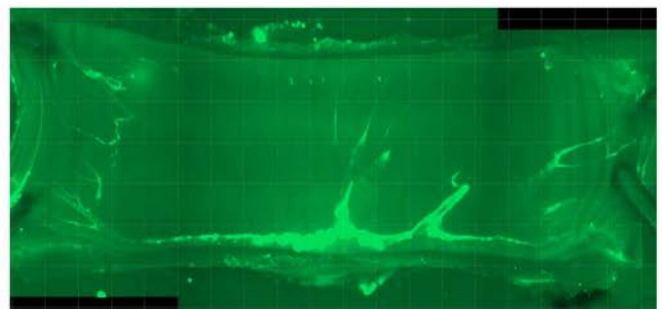
B *In vivo* Saline



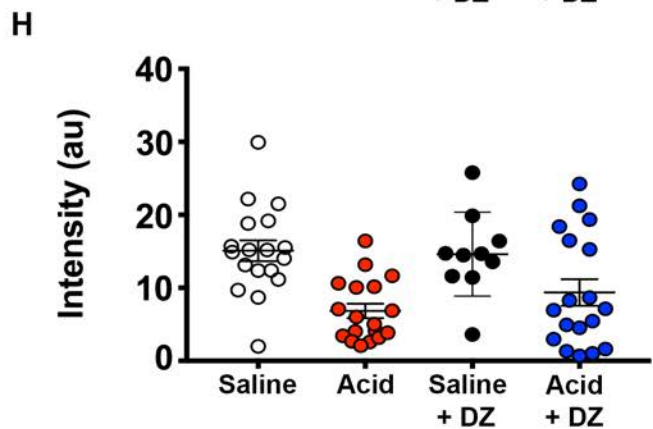
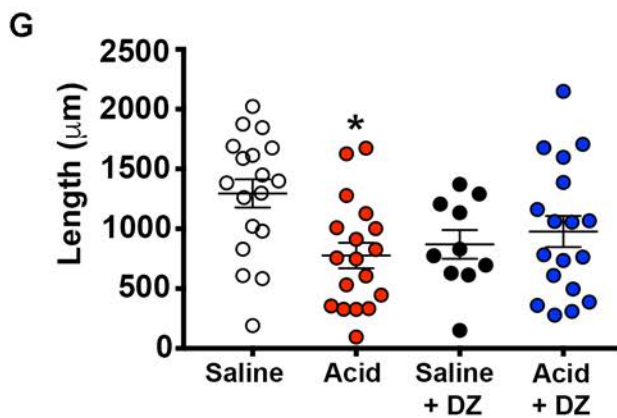
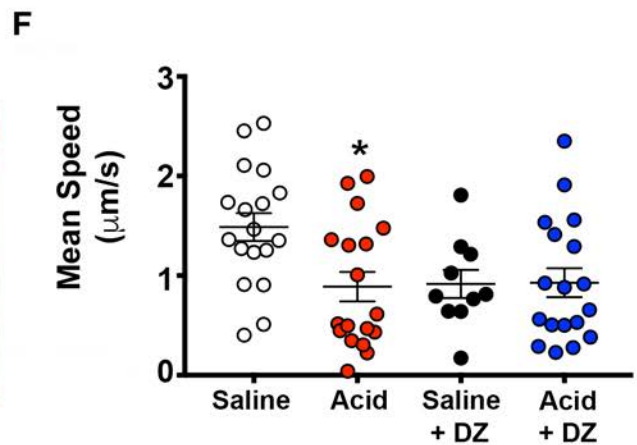
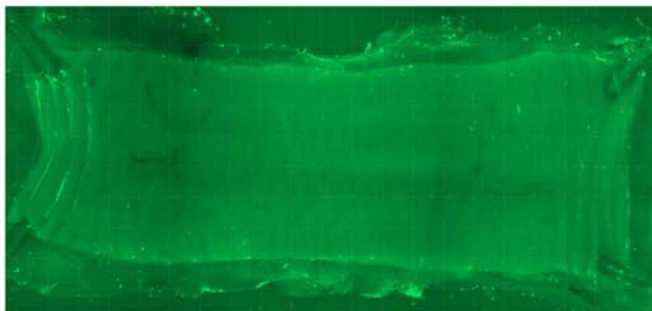
C *In vivo* Acid



D *In Vivo* Saline + Diminiazene Acetate



E *In Vivo* Acid + Diminiazene Acetate



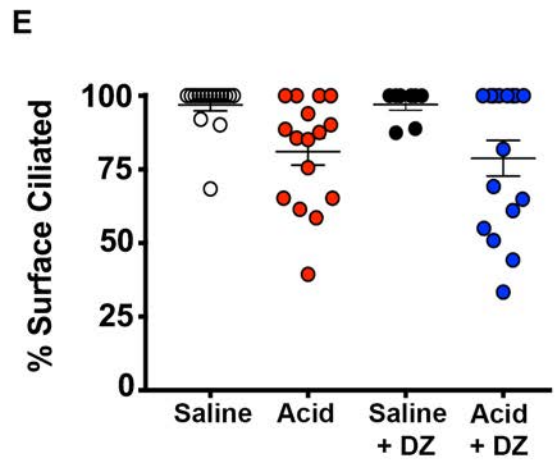
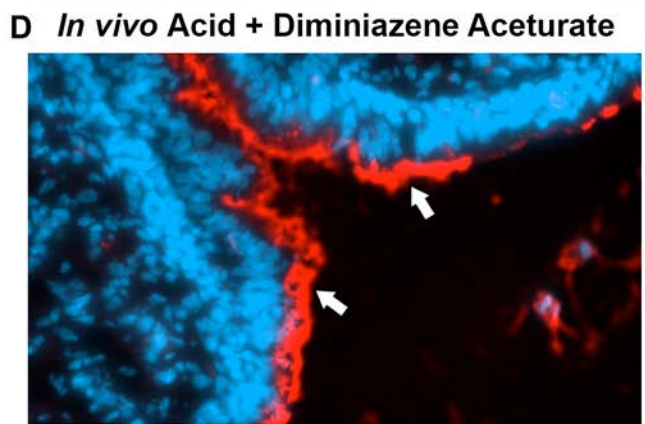
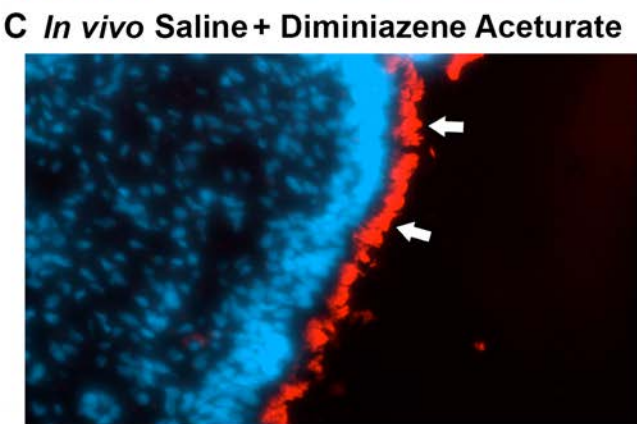
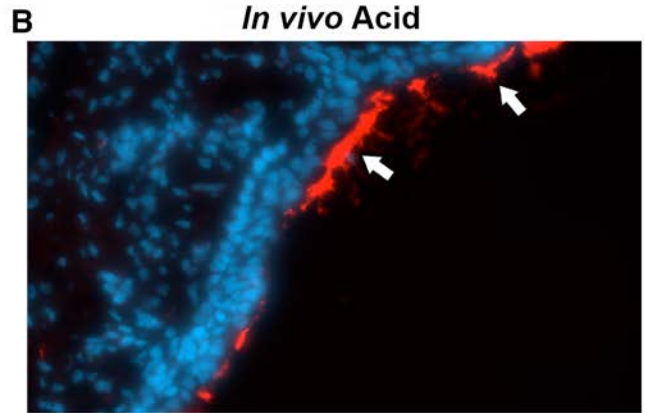
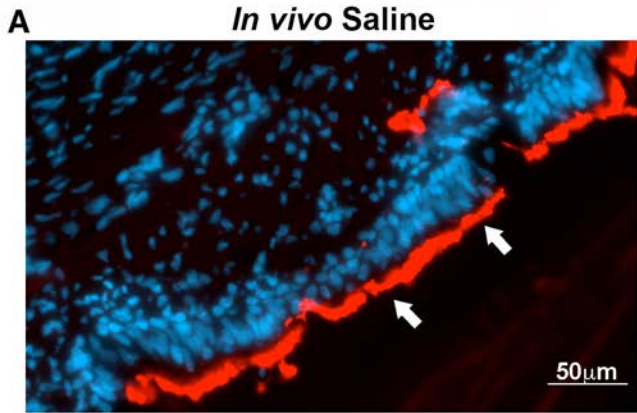


Table 1. Results separated by sex under non-stimulated or methacholine-stimulated conditions. Data are shown as Mean \pm SEM.

Variables	Groups								Two-way ANOVA P-values		
	Female				Male				Sex	Treatment	Sex* Treatment
	Female Saline	Female Acid	Female Saline + DZ	Female Acid + DZ	Male Saline	Male Acid	Male Saline + DZ	Male Acid + DZ			
<i>Under non-stimulated conditions</i>											
Bronchoalveolar lavage concentrations of MUC5AC	0.052 \pm 0.0045	0.071 \pm 0.0072	0.058 \pm 0.0071	0.064 \pm 0.0097	0.059 \pm 0.0076	0.064 \pm 0.0056	0.049 \pm 0.0084	0.047 \pm 0.0049	0.2749	0.2687	0.5291
Bronchoalveolar lavage concentrations of MUC5B	0.55 \pm 0.073	0.42 \pm 0.027	0.15 \pm 0.017	0.48 \pm 0.043	0.52 \pm 0.039	0.47 \pm 0.056	0.15 \pm 0.008	0.53 \pm 0.049	0.5560	<0.0001	0.7604
Surface MUC5AC mean signal intensity	111.7 \pm 11.52	110.4 \pm 10.75	84.44 \pm 8.48	125.8 \pm 9.91	94.38 \pm 7.97	87.77 \pm 8.04	79.05 \pm 4.71	87.29 \pm 9.32	0.0039	0.1159	0.4325
Surface MUC5B mean signal intensity	15.64 \pm 2.29	11.92 \pm 2.74	21.97 \pm 2.84	16.91 \pm 3.20	16.91 \pm 2.98	7.823 \pm 1.37	30.55 \pm 7.21	13.89 \pm 2.49	0.8849	0.0003	0.2582
Gland MUC5AC mean signal intensity	68.58 \pm 8.14	71.97 \pm 3.97	58.35 \pm 7.71	79.62 \pm 8.98	50.44 \pm 7.12	70.03 \pm 10.79	39.97 \pm 10.06	69.47 \pm 9.58	0.0559	0.034	0.7429
Gland MUC5B mean signal intensity	55.43 \pm 5.28	63.23 \pm 5.85	44.2 \pm 9.34	63.43 \pm 7.09	52.89 \pm 5.07	55.95 \pm 8.84	47.25 \pm 7.93	63.65 \pm 5.99	0.7426	0.1079	0.9023
Mean lung obstruction scores	1.44 \pm 0.18	2.22 \pm 0.28	1.8 \pm 0.37	1.56 \pm 0.24	1.33 \pm 0.17	2.33 \pm 0.24	1.40 \pm 0.25	1.67 \pm 0.17	0.6708	0.0011	0.7333
Mean percentage of trachea ciliated	100 \pm 0	89.81 \pm 4.17	96.86 \pm 3.14	75.02 \pm 9.84	93.81 \pm 3.91	72.22 \pm 7.03	97.20 \pm 2.79	82.51 \pm 7.54	0.4673	0.0033	0.2130
<i>Under methacholine-stimulated conditions</i>											
Bronchoalveolar lavage concentrations of MUC5AC	0.058 \pm 0.0035	0.059 \pm 0.0073	0.048 \pm 0.0059	0.058 \pm 0.0016	0.058 \pm 0.0035	0.054 \pm 0.0033	0.048 \pm 0.0074	0.054 \pm 0.0073	0.5453	0.2716	0.9659

Variables	Groups								Two-way ANOVA P-values		
	Female				Male				Sex	Treatment	Sex* Treatment
	Female Saline	Female Acid	Female Saline + DZ	Female Acid + DZ	Male Saline	Male Acid	Male Saline + DZ	Male Acid + DZ			
Bronchoalveolar lavage concentrations of MUC5B	0.63 ± 0.059	0.50 ± 0.023	0.14 ± 0.006	0.45 ± 0.011	0.63 ± 0.121	0.47 ± 0.008	0.15 ± 0.008	0.56 ± 0.031	0.5186	<0.0001	0.6148
Surface MUC5AC mean signal intensity	66.12 ± 15.34	39.98 ± 7.345	94.73 ± 7.075	77.52 ± 15.36	78.4 ± 9.44	69.19 ± 16.92	69.05 ± 13.6	83.36 ± 9.613	0.5620	0.1421	0.2151
Surface MUC5B mean signal intensity	13.79 ± 3.35	14.77 ± 6.38	57.12 ± 8.11	16.34 ± 4.85	19.06 ± 4.37	23.73 ± 10.53	81.42 ± 25.62	12.8 ± 1.02	0.2480	<0.0001	0.6511
Gland MUC5AC mean signal intensity	39.41 ± 8.16	38.92 ± 7.33	63.23 ± 10.25	45.17 ± 6.60	76.74 ± 6.20	54.81 ± 13.85	62.99 ± 10.84	39.41 ± 19.59	0.1231	0.2080	0.1771
Gland MUC5B mean signal intensity	32.24 ± 3.52	58.52 ± 15.89	77.1 ± 7.04	50.58 ± 15.41	36.86 ± 4.15	67.89 ± 14.55	109.9 ± 13.83	36.3 ± 8.52	0.3398	0.0002	0.3351
Mean lung obstruction scores	2.40 ± 0.24	3.25 ± 0.48	2.25 ± 0.48	2.00 ± 0.71	1.80 ± 0.31	3.18 ± 0.32	1.50 ± 0.29	2.00 ± 0.58	0.1645	0.0151	0.8601
Mean jacalin-labeled sheet index scores	1.81 ± 0.33	3.70 ± 0.26	1.40 ± 0.23	4.27 ± 0.43	1.45 ± 0.21	4.43 ± 0.16	1.98 ± 0.20	3.84 ± 0.34	0.5727	<0.0001	0.1370
Mean WGA-labeled sheet index scores	2.98 ± 0.66	4.08 ± 0.26	1.92 ± 0.48	4.18 ± 0.28	3.28 ± 0.76	3.98 ± 0.42	2.78 ± 0.39	4.63 ± 0.17	0.2365	0.0001	0.7673
Mean Jacalin-labeled strand index scores	1.60 ± 0.25	1.94 ± 0.37	1.16 ± 0.09	1.54 ± 0.13	1.53 ± 0.24	1.95 ± 0.18	1.03 ± 0.03	1.74 ± 0.25	0.9954	0.0175	0.8943
Mean WGA-labeled strand index scores	1.19 ± 0.11	1.83 ± 0.25	1.20 ± 0.13	1.83 ± 0.17	1.54 ± 0.22	2.04 ± 0.24	1.00 ± 0	1.53 ± 0.22	0.8631	0.0061	0.3713
Mean number of dilated submucosal gland ducts per mm ²	0 ± 0	1.86 ± 0.25	0 ± 0	4.42 ± 1.23	0 ± 0	3.79 ± 1.19	0 ± 0	5.45 ± 1.09	0.2557	<0.0001	0.6654

Variables	Groups								Two-way ANOVA P-values		
	Female				Male				Sex	Treatment	Sex* Treatment
	Female Saline	Female Acid	Female Saline + DZ	Female Acid + DZ	Male Saline	Male Acid	Male Saline + DZ	Male Acid + DZ			
Mean speed ($\mu\text{m/s}$) of mucus transport	1.32 \pm 0.22	0.90 \pm 0.19	0.93 \pm 0.22	0.71 \pm 0.14	1.66 \pm 0.16	0.87 \pm 0.23	0.89 \pm 0.20	1.15 \pm 0.24	0.2464	0.0103	0.5626
Mean length (μm) of mucus particle track	1162.0 \pm 201.0	789.7 \pm 168.7	816.7 \pm 141.5	680.6 \pm 115.0	1428.0 \pm 121.3	762.8 \pm 140.4	922.1 \pm 208.0	1273.0 \pm 191.7	0.0580	0.0117	0.2510
Mean intensity of fluorescently labeled mucus particles on the tracheal surface	14.46 \pm 1.08	7.21 \pm 1.37	17.41 \pm 2.53	9.44 \pm 2.55	15.71 \pm 2.71	6.46 \pm 1.51	11.82 \pm 2.13	9.28 \pm 2.74	0.4149	0.0103	0.5669